

## The Sensitivity of a Coupled Climate Model to Its Ocean Component

A. P. MEGANN, A. L. NEW, A. T. BLAKER, AND B. SINHA

*National Oceanography Centre, Southampton, United Kingdom*

(Manuscript received 25 August 2009, in final form 6 May 2010)

### ABSTRACT

The control climates of two coupled climate models are intercompared. The first is the third climate configuration of the Met Office Unified Model (HadCM3), while the second, the Coupled Hadley–Isopycnic Model Experiment (CHIME), is identical to the first except for the replacement of its ocean component by the Hybrid-Coordinate Ocean Model (HYCOM). Both models possess realistic and similar ocean heat transports and overturning circulation. However, substantial differences in the vertical structure of the two ocean components are observed, some of which are directly attributed to their different vertical coordinate systems. In particular, the sea surface temperature (SST) in CHIME is biased warm almost everywhere, particularly in the North Atlantic subpolar gyre, in contrast to HadCM3, which is biased cold except in the Southern Ocean. Whereas the HadCM3 ocean warms from just below the surface down to 1000-m depth, a similar warming in CHIME is more pronounced but shallower and confined to the upper 400 m, with cooling below this. This is particularly apparent in the subtropical thermoclines, which become more diffuse in HadCM3, but sharper in CHIME. This is interpreted as resulting from a more rigorously controlled diapycnal mixing in the interior isopycnic ocean in CHIME. Lower interior mixing is also apparent in the better representation and maintenance of key water masses in CHIME, such as Subantarctic Mode Water, Antarctic Intermediate Water, and North Atlantic Deep Water. Finally, the North Pacific SST cold error in HadCM3 is absent in CHIME, and may be related to a difference in the separation position of the Kuroshio. Disadvantages of CHIME include a nonconservation of heat equivalent to  $0.5 \text{ W m}^{-2}$  globally, and a warming and salinification of the northwestern Atlantic.

### 1. Introduction

To predict likely climate changes in the coming century, it is necessary to turn to numerical models, in which the atmosphere, ocean, and ice can be coupled together in a reliable manner. However, the projections of such coupled models for climate variables, such as the strength of the North Atlantic overturning circulation and atmospheric warming over the coming century, are widely different, as are the mechanisms involved. This was evident in the behavior of the models participating in the Intergovernmental Panel on Climate Change (IPCC) Third Assessment Report (Houghton et al. 2001). These models were forced with levels of atmospheric  $\text{CO}_2$  rising through the twenty-first century in a plausible Special Report on Emissions Scenarios (SRES) IS92 emissions scenario. While the models all showed a global atmospheric warming, some

showed substantial weakening of the Atlantic meridional overturning circulation (MOC) by the end of the century, some showed a modest reduction followed by stabilization, and one showed no significant reduction at all. A similar range of behavior was seen in the subsequent Fourth Assessment Report (Solomon et al. 2007). Such a spread in climate projections may be associated with differences in model resolution, in parameter choice, or in the representation of physical and dynamics processes. We may tentatively identify an additional contribution to uncertainty in climate projections as the vertical coordinate of the ocean component: the ECHAM4/Ocean Isopycnic Model (OPYC) in the Third Assessment and the Goddard Institute for Space Studies model EH (GISS-EH) and Bjerknes Centre for Climate Research Bergen Climate Model version 10 (BCCR BCM-2) in the Fourth Assessment all have an isopycnic (constant density) ocean, in contrast to the constant-depth coordinate used in almost every other model described in the Third and Fourth Assessment Reports. We note that the first two of these three models show little change in overturning over the twenty-first century, although the behavior of the

---

*Corresponding author address:* Dr. Alex Megann, National Oceanography Centre, Southampton, Empress Dock, Southampton SO14 3ZH, United Kingdom.  
E-mail: apm@noc.soton.ac.uk

third model is not distinguishable from the mean of the ensemble. The climate models included in the IPCC Assessments differ of course in many more aspects than in the vertical representation of their ocean components, and clearly no rigorous conclusion can be drawn from the behavior of these particular model simulations. Nevertheless, the use of ocean components that are structurally different from the standard Bryan–Cox type is a valuable tool toward understanding the structural biases associated with the choice of vertical coordinate of climate models.

For a coupled model to be suitable for climate change experiments it should as a minimum requirement perform well under constant, preindustrial atmospheric CO<sub>2</sub> concentrations in a “control” simulation. Clearly a degree of drift is unavoidable in such models, particularly in the deep ocean, where adjustment time scales of a century or longer are expected. In addition, the global mean surface temperature of a model initialized with late-twentieth-century ocean conditions, but forced with preindustrial atmospheric gas concentrations, would be expected to be about 0.3° cooler than present-day climatologies (Houghton et al. 1996). Nevertheless, we expect a model to reach an acceptably steady climate within a few decades that is stable, both in terms of its net top-of-atmosphere (TOA) radiation and ocean surface fields, and having a rate of drift of temperature and salinity that is low compared with those typical of climate change scenarios. The quasi-steady state of the simulated climate should in addition be in reasonable agreement, subject to the above caveats, with that currently observed, including realistic air–sea fluxes, ocean circulation, and heat transports.

The third climate configuration of the Met Office Unified Model (HadCM3) coupled model (Gordon et al. 2000, hereafter G2000), developed at the Hadley Centre for Climate Prediction and Research (part of the Met Office), is one of the models included in the climate change experiments described in the IPCC Third and Fourth Assessment Reports, and has been shown to have a remarkably stable climate when forced with preindustrial greenhouse gas concentrations. The global mean ocean surface temperature error remains within 0.2°C of climatological estimates over more than four centuries, despite the absence of any flux correction. The ocean circulation is also broadly in agreement with reality, with appropriate caveats concerning its relatively coarse (1.25°) horizontal resolution. There remain, however, a few significant errors in the ocean component of HadCM3, including a cold error of up to 4°C over a large area of the North Pacific; progressive surface freshening; slow drifts in the temperature and salinity below 1000-m depth; and changes in the meridional overturning circulation over

centennial time scales, with the southward flow of North Atlantic Bottom Water occurring at increasingly shallower depths.

Isopycnic (density coordinate) models such as the Miami Isopycnic-Coordinate Ocean Model (MICOM; Bleck and Smith 1990) eliminate by design spurious diapycnal mixing in the advection scheme, and their use in ocean-only simulations has led to the identification of specific advantages over the more traditional depth-coordinate models. These include better representations of near-adiabatic flows along sloping isopycnals, such as the Equatorial Undercurrents (Megann and New 2001) and deep western boundary currents; the absence of spurious numerical mixing of dense waters at sill overflows (Roberts et al. 1996); and the preservation of water properties over long time and length scales (Marsh et al. 1996). Although this type of model also has some significant disadvantages, including reduced vertical resolution in regions of low stratification, such as the Arctic, and imprecisely defined detrainment from the mixed layer, they have at least the potential to illuminate the effects of changing the vertical coordinate of the ocean.

To attempt to evaluate unambiguously the effects of changing the vertical representation in an ocean model, a well-controlled experimental procedure must be followed, in which the bathymetry, resolution, initialization, and surface forcing fields are as close as possible between the two models being compared. Two notable intercomparison projects involving ocean-only implementations of *z*-coordinate and isopycnic models of the Atlantic have followed such procedures. These are the Atlantic Isopycnic Model (AIM) project (Roberts et al. 1996; Marsh et al. 1996) and the Dynamics of North Atlantic Models (DYNAMO) project (New et al. 1995; New and Bleck 1995; Willebrand et al. 2001). These studies revealed significant differences in the pathway of the North Atlantic Current (NAC) between the model types, with the NAC in the *z*-coordinate and terrain-following models taking an unrealistically zonal pathway across the basin farther south than that observed, but occupying a more realistic path in the isopycnic model. This shift in NAC position was attributed by Roberts et al. (1996) to excessive levels of mixing in the deep outflows from the Nordic seas, in turn leading to the formation of a vertically homogeneous water mass in the North Atlantic subpolar gyre. An intercomparison experiment was also carried out by Chassignet et al. (1996) with results broadly consistent with those of Roberts et al. (1996). In all these experiments the path of the NAC in the isopycnic-coordinate models lies closer to reality, and deep water masses are more faithfully represented and preserved in the isopycnic models. A further near-global ocean-only intercomparison using the Global Isopycnic Model (GIM)

was carried out by Megann and New (1995), which in addition found similar differences in the path of the Kuroshio and North Pacific Current (NPC). Specifically, the Kuroshio separated farther north in the isopycnic model to form an NPC centered at about 38°N, in contrast to the  $z$ -coordinate model, in which the main separation and NPC pathway occurred at 32°N (in contrast with the observed Kuroshio separation at approximately 35°N).

In the Hybrid-Coordinate Ocean Model (HYCOM; Bleck 2002), the ocean interior is represented by layers of constant potential density, as in MICOM, but light layers that would outcrop and disappear in a pure isopycnic model are reused as constant-depth, near-surface coordinate levels with specified minimum thicknesses. It is therefore largely an isopycnic ocean model and can be viewed as the direct successor to MICOM, while reducing the main deficiency of the latter; namely, the loss of resolution in weakly stratified regions. Its suitability for ocean modeling studies has been confirmed by Sun and Bleck (2001a) and Halliwell (2004), and it has also been successfully coupled to an atmospheric model (Sun and Bleck 2001b, 2005). The following shortcomings, nevertheless, remain in HYCOM: the use of potential, rather than in situ, density means that regardless of the reference pressure chosen the vertical coordinate cannot be monotonic with depth everywhere, and there are residual pressure gradient errors resulting from the temperature dependence of the compressibility, even though this can be corrected to at least first order (Sun et al. 1999). The transition between isopycnic and constant-depth regimes may lead to numerical diffusion (R. Bleck 2002, personal communication), and at high latitudes the vertical resolution may still be limited, as in MICOM. Finally, Asselin time filtering associated with the two-level time stepping used in HYCOM (though not in all isopycnic models) causes a nonconservation of tracers that may be of significant magnitude in climate models.

In this paper we present results from a control simulation of the Coupled Hadley–Isopycnic Model Experiment (CHIME). This has the same atmosphere and ice models as HadCM3 and the same ocean resolution over most of the globe, but uses the hybrid-coordinate ocean model HYCOM instead of the conventional constant-depth vertical coordinate system used in HadCM3. Although it could be argued that the resolution of the HadCM3 grid and its numerics fall short of the current state-of-the-art models, the present comparison is nevertheless of interest, since HadCM3 is still widely used in climate studies. This is the first time, to our knowledge, that such a direct comparison has been undertaken between coupled models with structurally different ocean components. The fact that the two models are identical

apart from their ocean component allows us the possibility of establishing whether specific characteristics of HadCM3 arise intrinsically from the ocean or atmosphere components of the model. A secondary goal of this study is to assess the long-term stability of the CHIME coupled climate model and assess its performance against that of HadCM3. We would expect that the vertical diffusion in the ocean components of the two models will be significantly different, resulting in different drifts in the ocean interior. In particular, we will test the hypothesis that heat and salt will diffuse downward below the 300–800-m depths typical of subtropical gyre thermoclines more rapidly in the  $z$ -coordinate ocean of HadCM3.

In section 2 the CHIME coupled model is described. In section 3 we examine the heat transport, the meridional overturning circulation and the annual cycle of ice cover in each model. In section 4, we address the surface temperature and salinity errors and the oceanic circulation, and compare the mixed layer depths of the models with fields derived from climatology. In section 5 we discuss the respective abilities of the two models to preserve the integrity of their water masses, and relate these to the vertical coordinate system used in each model. The representation of the subtropical thermoclines in the two models will be discussed and compared against observations. In section 6 we summarize the results and discuss likely mechanisms for the differences between the two models.

## 2. Model description and initialization

The atmosphere and sea ice models of CHIME are taken from HadCM3, with atmospheric parameters identical to those used in the control experiment aaxzc of the latter. As is the case in HadCM3, no flux adjustment is applied to the air–sea coupling. The atmospheric component is described in detail in G2000. In brief, it has a spherical grid with cell sizes 3.75° east–west and 2.5° north–south, and uses a hybrid vertical coordinate with 19 vertical levels. The sea ice model (Cattle and Crossley 1995) is a simple thermodynamic model, plus ice drift with the ocean surface current, and with partial ice coverage to allow representation of leads. The three scalar prognostic fields of the sea ice model are ice thickness, fractional ice cover, and snow depth. The advection and diffusion scheme in the sea ice model are recoded for consistency with the Arakawa C grid used for the CHIME ocean model, the HadCM3 ocean being defined on a B grid.

The ocean model is version 2.1.34 of HYCOM (Bleck 2002). In the interior, which in the present model configuration constitutes more than 93% of the ocean domain by volume, the vertical coordinate is close to isopycnic

over the whole annual cycle. However, in near-surface waters, or wherever a prescribed layer density is not present in any given water column, the layers that would be unused in a purely isopycnic model are constrained to have a minimum thickness and their density is allowed to vary. In the present implementation, the minimum thickness of the surface layer is 5 m, while the minimum thicknesses of subsurface layers increases to a maximum of 15 m by layer 5. The vertical coordinate is potential density referred to a pressure of 2000 dbar, and the thermobaric correction to the pressure gradient of Sun et al. (1999) is applied. If the density in a given grid cell changes as a result of mixing, HYCOM adjusts the depth of the upper or lower interface of each layer to return the density toward the reference density of that layer; in the experiment described here this regridding process is carried out using a piecewise linear mapping (PLM) algorithm. The reference densities for the 25 layers (Table 1) were chosen to resolve the major water masses of the global ocean, with enhanced resolution at low densities to improve the accuracy of the mixing scheme in the mixed layer. The CHIME ocean therefore has more layers than the 20 used in HadCM3; the extra five layers, however, are concentrated at low densities, and do not change the density resolution in the interior, for instance in the thermocline region (although this does of course give CHIME more near-surface resolution in high latitudes than if it only had 20 layers).

The east–west filtering procedure used in HadCM3 to prevent violations of the CFL stability criterion at latitudes poleward of 75°N is inappropriate in a layer model such as HYCOM, where layer thickness is required to be positive definite, so the spherical grid used throughout HadCM3 is not useable in the Arctic in CHIME. The ocean model therefore uses a spherical-bipolar grid similar to that described by Sun and Bleck (2001a), and is composed of two regions. The first, extending from 55°N to the southern boundary at 78°S, has constant angular resolution of 1.25° in both north–south and east–west directions, and the mass points in this domain are exactly coincident with those of the HadCM3 ocean model grid. North of 55°N the spherical grid is matched smoothly to a bipolar grid, which avoids problems caused by the convergence of meridians toward the North Pole. The poles of the bipolar grid are situated well inland at 55°N, 110°W, and 70°E, and the resolution at ocean points north of 55°N is between 40 and 140 km; the polar island used in HadCM3 is therefore avoided with this grid. Over the spherical part of the grid there are exactly six ocean grid cells underlying each atmospheric cell, as is the case with HadCM3.

The bathymetry and coastlines used in CHIME are shown in Fig. 1. The bathymetry is derived from Sandwell

TABLE 1. Layer target densities and minimum thicknesses in CHIME.

$k$	$\sigma_k$	$\Delta z_k^0$ (m)
1	29.60	5.0
2	30.20	7.0
3	30.80	9.8
4	31.40	13.7
5	32.00	15.0
6	32.60	15.0
7	33.20	15.0
8	33.80	15.0
9	34.40	15.0
10	35.00	15.0
11	35.30	15.0
12	35.60	15.0
13	35.85	15.0
14	36.05	15.0
15	36.25	15.0
16	36.45	15.0
17	36.60	15.0
18	36.75	15.0
19	36.86	15.0
20	36.96	15.0
21	37.04	15.0
22	37.12	15.0
23	37.20	15.0
24	37.32	15.0
25	37.44	15.0

and Smith (1997), interpolated onto the model mass grid. A minimum depth of 100 m is then imposed everywhere to prevent numerical barotropic instabilities in shallow water (HadCM3, by comparison, has a minimum depth of 139 m). Use of the bipolar grid in the Arctic means that the locations of grid points, and hence of the coastlines, in this region cannot be identical to those in HadCM3, so in CHIME the coastlines are defined everywhere at the ocean resolution, where in HadCM3 coastlines are at the coarser atmospheric resolution. The coastlines are at first defined to be the zero-depth contour after interpolation, and are then adjusted to ensure critical straits remain open to a realistic depth. The bathymetry was excavated in the North Atlantic so that the sills between Greenland and Scotland have a minimum depth of 800 m, resulting in comparable sill depths to those in HadCM3. The Bering and Gibraltar straits are both open in CHIME, and are represented by channels a single grid cell wide. The continuity of the computational grid across Bering Strait is ensured by explicitly copying all prognostic fields into “shadow zones” on each side of the strait. This is in contrast to HadCM3, in which the numerical B grid of the ocean model prohibits flow through single-gridpoint channels; in the latter model there is no barotropic flow through Bering Strait, and an exchange algorithm is used to simulate the exchange flow at Gibraltar Strait. Because the coastlines in CHIME do not correspond exactly to the

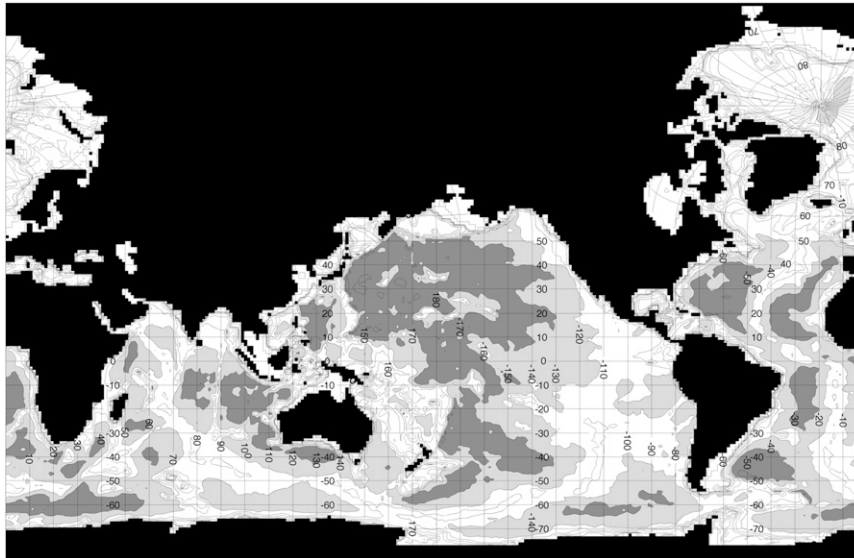


FIG. 1. CHIME bathymetry: gray shading denotes depths  $>3000$  m; dark gray denotes depths  $>5000$  m.

atmospheric grid north of  $55^{\circ}\text{N}$ , a coastal tiling and interpolation scheme identical to that used by Sun and Bleck (2001a) is employed to conserve fluxes passed between the atmosphere and ocean. To avoid spurious maxima in the wind stress curl, the wind stress passed from the atmosphere to the ocean is linearly interpolated between the centers of each atmospheric cell. The ocean and ice fields are coupled daily to the atmosphere using the OASIS 2.4 coupler (Valcke et al. 2000).

The K-profile parameterization (KPP) diapycnal mixing scheme (Large et al. 1994) is used in CHIME, which was found by Halliwell (2004) to afford superior performance to the Kraus–Turner bulk mixed layer scheme when used with HYCOM. This is significantly different from the bulk mixed layer scheme and the Pacanowski and Philander internal mixing parameterization used in HadCM3, and we note that this introduces an additional difference between the two ocean models besides the vertical coordinate. The critical HYCOM parameter values used for this scheme in CHIME are background internal wave viscosity  $\text{difmiw} = 1 \times 10^{-4} \text{ m}^2 \text{ s}^{-1}$ , background internal wave diffusivity  $\text{difsiw} = 1 \times 10^{-5} \text{ m}^2 \text{ s}^{-1}$ , and the critical bulk Richardson number  $\text{ricr} = 0.45$ . Initial sea ice cover was taken from estimates of Gloersen et al. (1993), and the initial thickness of sea ice in all ice-covered grid cells was set to 2 m. The atmospheric initial state was identical to that in the HadCM3 control run described in G2000. The model was initialized from the full-depth Levitus et al. (1998) autumn climatology, projected onto the model density layers, and run in fully coupled mode for 200 years from rest. Atmospheric forcing was with

preindustrial levels of greenhouse gases and aerosols. We shall use the same averaging period as in G2000; namely, years 80–119, to allow direct comparisons to be made between the two models.

### 3. Large-scale diagnostics

#### a. Global mean diagnostics

The global mean top-of-atmosphere radiation in CHIME settles, by year 60, to a mean value of about  $+0.2 \text{ W m}^{-2}$  in the downward direction, implying a long-term warming of the ocean. This can be compared with the long-term mean in HadCM3 (shown in Fig. 2 of G2000), which is of similar magnitude but of negative sign (in other words, a net cooling of the ocean). The interannual and decadal variability of the TOA flux in CHIME are similar to that in HadCM3, with the variance of the annually averaged mean radiation  $0.30 \text{ W m}^{-2}$ . Figure 2a shows the global (mass weighted) mean ocean potential temperature in the two models. It should be noted that the discrepancy in the global mean temperature at initialization between the two models ( $3.61^{\circ}\text{C}$  in CHIME and  $3.46^{\circ}\text{C}$  in HadCM3) is due to the different coastlines used in each case and differences in bathymetry related to the different vertical coordinate. The mean rate of cooling in the second century of CHIME is  $0.06^{\circ}\text{C century}^{-1}$ , equivalent to a surface heat loss of  $0.3 \text{ W m}^{-2}$ , while in the same period HadCM3 cools at a rate of  $0.016^{\circ}\text{C century}^{-1}$ , equivalent to a global mean surface heat loss of about  $0.08 \text{ W m}^{-2}$ . We have noted that HYCOM is known not to conserve heat and salt exactly because of nonadiabatic time

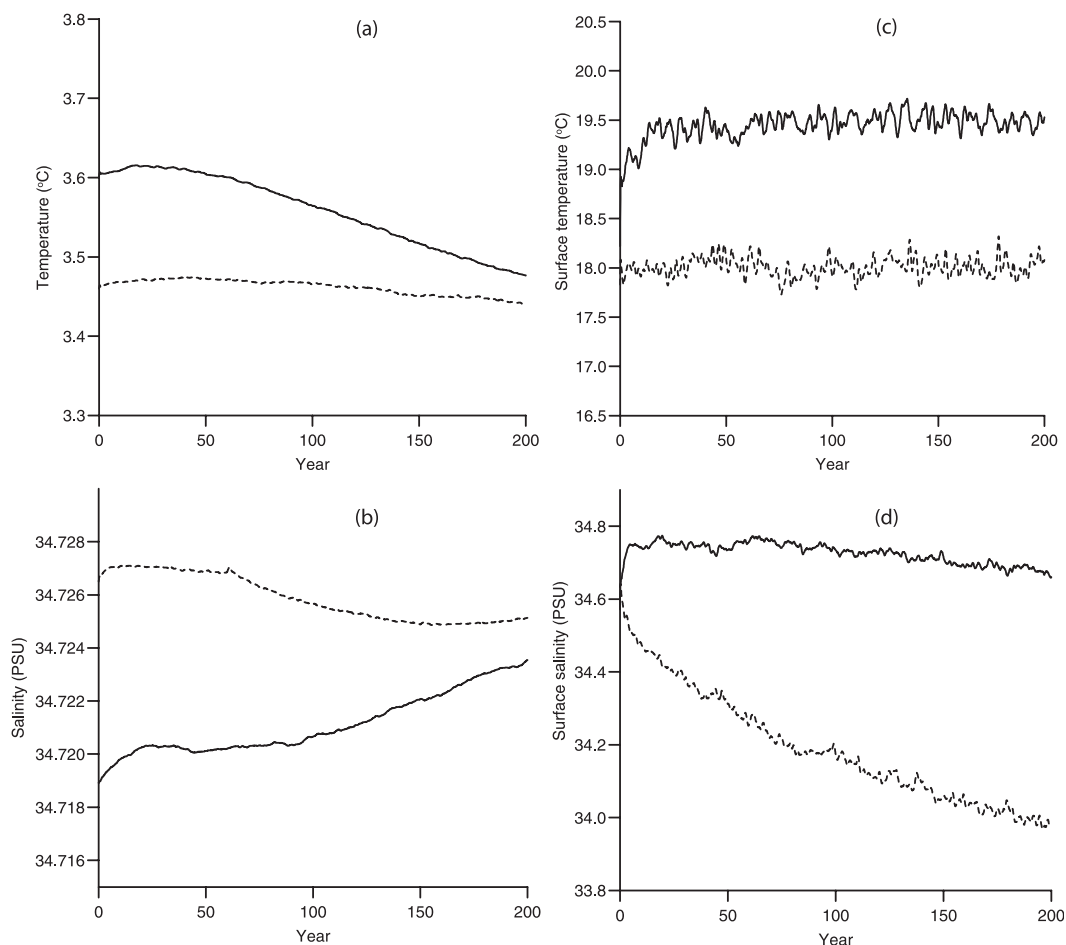


FIG. 2. Global mean ocean fields in CHIME (solid lines) and HadCM3 (dashed lines): (a) potential temperature, (b) salinity, (c) sea surface temperature, and (d) sea surface salinity.

smoothing of layer interfaces in the continuity equation. The actual amount of nonconservation depends on the length of the time step and on the level of short-time-scale variability. In CHIME the internal nonconservation is equivalent in a global mean to a surface heat loss of about  $0.5 \text{ W m}^{-2}$ , equivalent to a global mean tendency of  $0.1^\circ\text{C century}^{-1}$ , which accounts for the discrepancy between the TOA imbalance and the rate of change of the ocean heat content in Fig. 2a. It should be noted that this deficiency arises from the time-stepping scheme in HYCOM, rather than from the vertical coordinate, and that at least one isopycnic model (GOLD) indeed conserves heat and salt to within roundoff errors (Hallberg and Adcroft 2009). Recent developments in HYCOM (R. Bleck 2009, personal communication; M. Bentsen 2009, personal communication) address this deficiency and promise to reduce it by up to an order of magnitude. This internal loss could have been reduced by using a shorter time step than the 36 min used here but, for the sake of practical run times, was judged to be acceptable

in this application. For comparison, the present radiative effect of anthropogenic greenhouse gases is estimated in the IPCC Fourth Assessment Report to be  $1.6 \pm 0.9 \text{ W m}^{-2}$ .

Figure 2b shows the global mean salinity in the two models. The discontinuity at year 60 in HadCM3 is associated with the imposition of upper and lower limits on the salinity in inland seas. In CHIME the global mean changes little for the first 80 years, and then rises at about  $0.003 \text{ psu century}^{-1}$ , equivalent to a global evaporation of  $2.5 \text{ mm yr}^{-1}$ . Figure 2c shows the global mean sea surface temperature (SST) in CHIME and HadCM3. The mean SST in CHIME starts at  $18.22^\circ\text{C}$  (the difference from HadCM3 is again due to the different coastlines) and rapidly warms by about  $1.3^\circ\text{C}$  in the first 20 yr; much of this error is located in the Southern Ocean, where it is due to the shallow bias in summer mixed layer depths, which will be described below, but there are also extensive areas of warm error in the North Atlantic and the tropics. Figure 2d shows the global mean surface salinity (SSS) in CHIME and HadCM3. In CHIME, the mean SSS rises a little in the

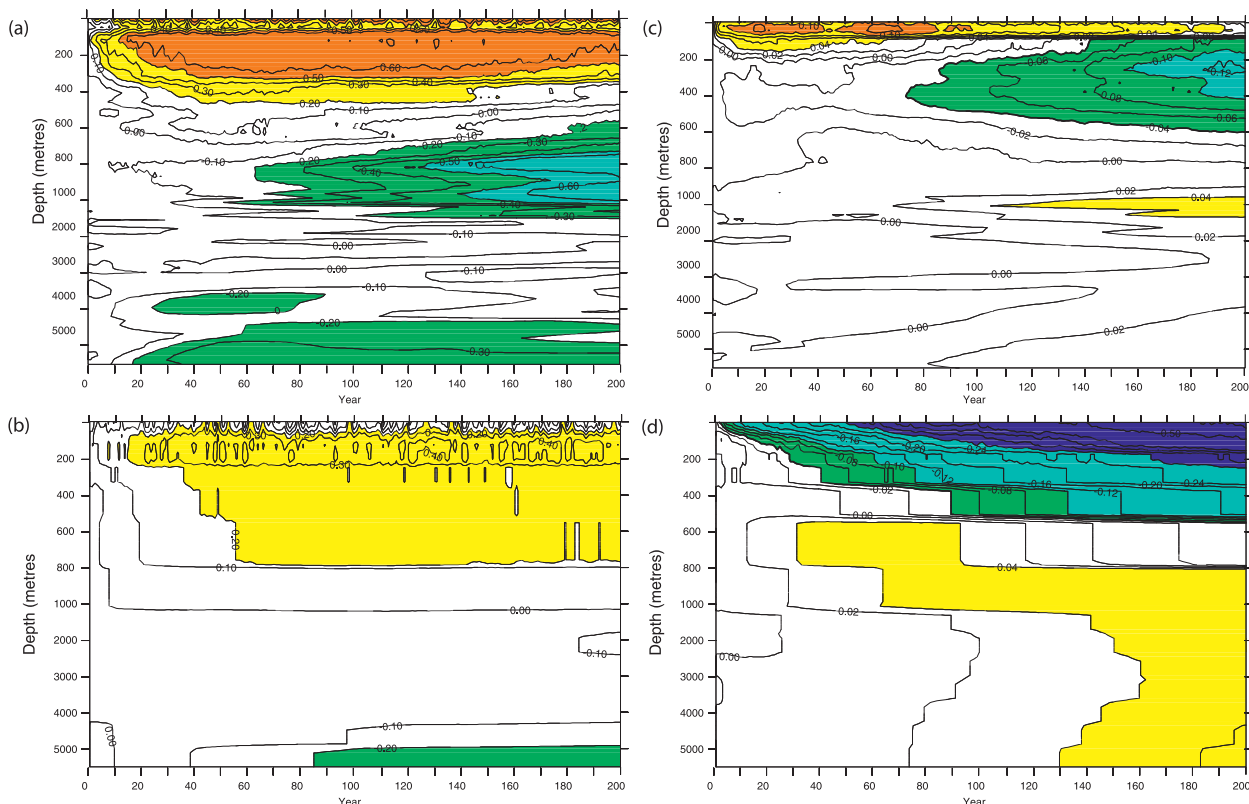


FIG. 3. Drift of the global mean ocean temperature ( $^{\circ}\text{C}$ ) in (a) CHIME and (b) HadCM3 as a function of depth, relative to the initial state, and drift of the global mean salinity (PSU) in (c) CHIME and (d) HadCM3.

first five years, mainly in the Northern Hemisphere subtropical gyres, and then falls slowly to a value similar to that at initialization by years 200. In HadCM3 there is an initial rapid decrease, which reduces after a few decades but continues to drop for at least 200 years; a similar drift is also seen in the related HadCEM (Roberts et al. 2004) and HadGEM1 (Johns et al. 2006) coupled models.

In Figs. 3a,b, we show the drift of the global mean temperature in CHIME and HadCM3 as a function of depth, relative to the initial state. This corresponds directly to Fig. 3a of G2000, although the latter has a longer time axis and smoothed contours. There is a significant difference between the two models at the surface, as already noted, with the global mean surface temperature error in HadCM3 remaining less than  $0.1^{\circ}\text{C}$  for the whole 200 years, while CHIME shows a global warm bias, with a mean surface error of a little over  $1^{\circ}\text{C}$  developing by year 30, and remaining stable thereafter. In both HadCM3 and CHIME there is a subsurface warming that, starting from just below the surface, gradually extends to deeper depths over the next few decades (although Fig. 3a of G2000 indicates that the subsurface warming in that model at least partially reverses after year 200). The warming has a maximum at around 200 m of around  $0.5^{\circ}\text{C}$  in HadCM3

and  $0.7^{\circ}\text{C}$  in CHIME. In CHIME the warming reaches only 500–600 m, while in HadCM3 it extends to 800–1000 m. Farther down, both models cool: in CHIME the maximum cooling is between 800- and 1500-m depth and reaches  $0.6^{\circ}\text{C}$  by year 200, while in HadCM3 the cooling is only slight ( $0.1^{\circ}\text{--}0.2^{\circ}\text{C}$ ) and occurs below 1500 m. We remark here that the main thermocline in subtropical regions typically exists in the depth range of 300–800 m. While the globally averaged drifts are clearly driven by different processes in different regions, it does raise the possibility that the subtropical thermoclines in HadCM3 are becoming warmer, and extending more deeply as time progresses (and possibly more diffuse, though this figure is inconclusive), whereas the warming–cooling dipole with a zero near 600–800 m in CHIME implies that subtropical thermoclines are better maintained, or even increasing their vertical gradients. This is discussed in more detail below.

The drift of global mean salinity as a function of depth in the two models is shown in Figs. 3c,d. In the upper 150 m, CHIME initially becomes saltier, unlike HadCM3, which freshens steadily (and continues to freshen in the upper ocean at least as far as 500 years). The global mean surface salinity in CHIME increases by 0.1 psu in the first

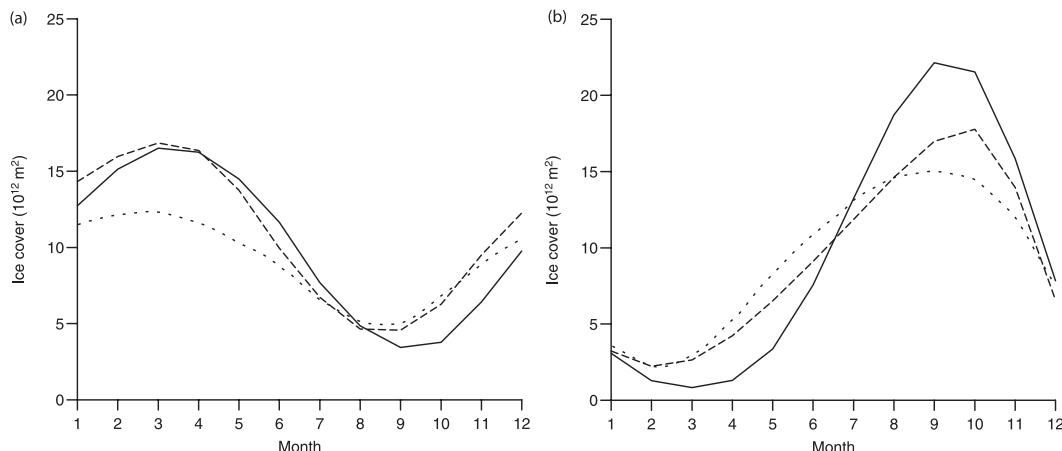


FIG. 4. Mean annual cycle of total ice area in (a) the Northern Hemisphere and (b) the Southern Hemisphere. The ice cover in CHIME is shown by the solid line; that in HadCM3 by a dashed line; and in the SSM/I climatology by a dotted line.

decade and then drops back close to the initial value by year 200; that in HadCM3 drops by 0.54 psu over the same period. Below 1000 m, the salinity drift in CHIME is rather less than in HadCM3, where the deep salinity continues to increase at around  $0.03 \text{ psu century}^{-1}$  until beyond year 400 of the run (shown in Fig. 3b of G2000). The most significant drift in CHIME is the freshening between 150 and 600 m, which extends less deeply than that in HadCM3, reaching 600 m where in the latter it reaches 1000 m. In HadCM3 the upper-ocean freshening occurs throughout the Atlantic and Arctic, with the salinity increasing at depth, but in the Pacific and Southern oceans the deeper increase does not happen and the surface fresh anomaly propagates steadily downward. The pronounced salinity decrease above 500–600 m in HadCM3 and increase deeper down, points to the possibility of excessive diapycnal mixing in the subtropical thermocline regions (in which salty water above the thermocline overlies fresher waters below).

#### b. Ice cover

The values of the basal heat flux diffusivity eddydiff in each hemisphere were tuned in the first decade or two in CHIME, to give good agreement in the annual means of hemispheric ice cover with HadCM3 (and hence with observations) to avoid the effect of large changes in ice cover on surface fluxes and the radiation balance. It should be noted that these parameter values will be different from those in HadCM3 because of differences in the surface temperature, especially given the warm bias in the Southern Ocean in CHIME. For this reason, the annual mean hemispheric ice cover is not a revealing diagnostic in CHIME, but it is nevertheless of interest to compare the annual cycle of the ice cover.

Figure 4 shows the mean annual cycle of ice area in CHIME, averaged over each hemisphere, superposed on the observed [Special Sensor Microwave Imager (SSM/I)] curve as shown in Fig. 10 of G2000. The winter cover in the Northern Hemisphere in CHIME (Fig. 4a) is similar to that in HadCM3, although the summer minimum of  $4.0 \times 10^{12} \text{ km}^2$  is deeper in CHIME than that in HadCM3 ( $4.9 \times 10^{12} \text{ km}^2$ ). In the Southern Hemisphere (Fig. 4b), the mean cover is similar in the two models, but it is evident that the annual range of ice cover is substantially higher in CHIME than in HadCM3: these are  $21.3 \times 10^{12} \text{ km}^2$  and  $15.6 \times 10^{12} \text{ km}^2$ , respectively. The annual range in both hemispheres in both models is rather larger than those in observations; in particular, the maximum Arctic winter ice cover is over 40% higher in both HadCM3 and CHIME than observed, and in the Antarctic HadCM3 has 15% and CHIME over 50% more ice cover, while CHIME has rather less ice in the summer than either HadCM3 or observations. However, the fact that the wintertime ice cover is greater in CHIME than in HadCM3 or in the observations is likely to reduce the amount of winter heat loss, and hence potentially the production of dense bottom water.

#### c. Oceanic heat and mass transports

In Fig. 5, we show the global northward oceanic heat transport in years 80–119 of CHIME and HadCM3, along with climatological estimates by Ganachaud and Wunsch (2000) and by Trenberth and Caron (2001). In the extratropics the heat transport in the two models are rather similar, while in the tropics CHIME carries less heat northward than HadCM3. Both models are in good agreement with the observational estimates at  $32^\circ\text{S}$ ,  $19^\circ\text{S}$ , and  $48^\circ\text{N}$ , but both carry less heat at  $24^\circ\text{N}$  than that

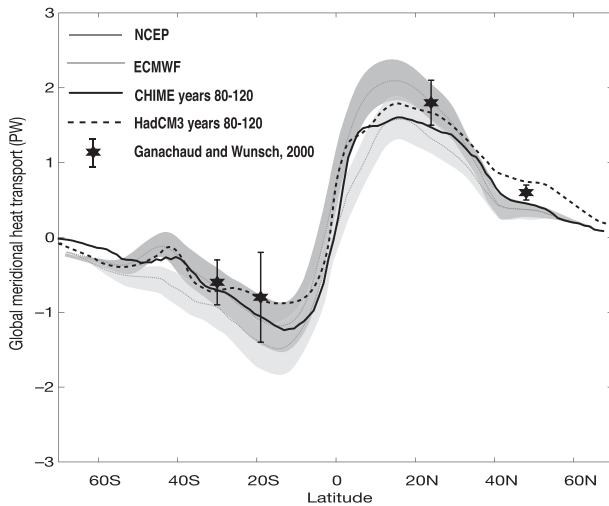


FIG. 5. Global mean ocean heat transport in PW in CHIME (solid curve) and HadCM3 (dashed curve). The stars show the estimates of Ganachaud and Wunsch (2000). The dotted lines are from the reanalysis of Trenberth and Caron (2001): the darker gray shading denotes the confidence limits of estimates based on National Centers for Environmental Prediction (NCEP) fluxes, while the light gray shading corresponds to estimates based on European Centre for Medium-range Weather Forecasts (ECMWF) fluxes.

estimated by Ganachaud and Wunsch (2000). North of 40°N both CHIME and HadCM3 carry more heat than the mean of the observational estimates, and north of 50°N the northward transport in CHIME is stronger than in HadCM3. Overall, however, the global heat transports in both models are generally within the error bars of the observational estimates.

Table 2 shows the meridional ocean heat transports across selected sections in years 80–119 of CHIME and HadCM3, along with the climatological estimates of Ganachaud and Wunsch (2000). In the North Atlantic, CHIME and HadCM3 transport 0.54 and 0.53 PW at 48°N and 0.97 and 1.14 PW, respectively, at 24°N; at the former section Ganachaud and Wunsch estimate a rather larger 1.3 PW, although G2000 refer to previous climatological estimates of 1.1 and 1.2 PW. The divergences of the heat transports imply that CHIME gains more heat from the atmosphere south of 24°N than HadCM3 and loses less heat between 24° and 48°N, although the differences are around 0.1 PW, which is of the same order as the error estimates of the transports. In the North Pacific, Ganachaud and Wunsch estimate northward transports of 0.5 PW at 24°N and 0 PW at 48°N, while the corresponding transports in CHIME are 0.44 and 0.08 PW and in HadCM3 are 0.50 and 0.17 PW, so the CHIME heat transports at 24°N lie within observational bounds.

The Atlantic meridional overturning streamfunctions, averaged over years 80–119, are shown in Fig. 6. The overturning circulation is again similar in the two models,

TABLE 2. Meridional ocean heat transports (PW) across selected sections in CHIME and HadCM3, along with the climatological estimates of Ganachaud and Wunsch (GW2000).

	CHIME	HadCM3	GW2000
Atlantic 48°N	0.53 ± 0.09	0.54	0.60
Atlantic 24°N	0.97 ± 0.10	1.14	1.30
Atlantic 18°S	0.31 ± 0.11	0.67	0.90
Atlantic 34°S	0.33 ± 0.08	0.60	0.30
Indian 18°S	−1.67 ± 0.11	−1.84	−1.80
Indian 34°S	−1.41 ± .08	−1.60	−1.50
Pacific 48°N	0.08 ± 0.01	0.17	0.00
Pacific 24°N	0.44 ± 0.06	0.50	0.50
Pacific 18°S	0.34 ± 0.29	0.33	0.20
Pacific 34°S	0.43 ± 0.09	0.41	0.60

with a maximum of 18–20 Sv ( $1 \text{ Sv} \equiv 10^6 \text{ m}^3 \text{ s}^{-1}$ ) at a depth of 800–1000 m in both cases, which, after a spinup period of 60–80 years, is stable to within about 10% at least as far as year 200. There is no single local maximum in either model, but maxima of between 18 and 20 Sv occur between 25° and 50°N in both. The densest overflow waters in CHIME sink more deeply than in HadCM3: the 4-Sv contour reaches 3800 m in the former and 3200 m in the latter. At most latitudes in the North Atlantic south of 40°N, the southward-flowing North Atlantic Deep Water (NADW) lies deeper in CHIME than in HadCM3 (possible reasons for which are discussed below); the 10-Sv

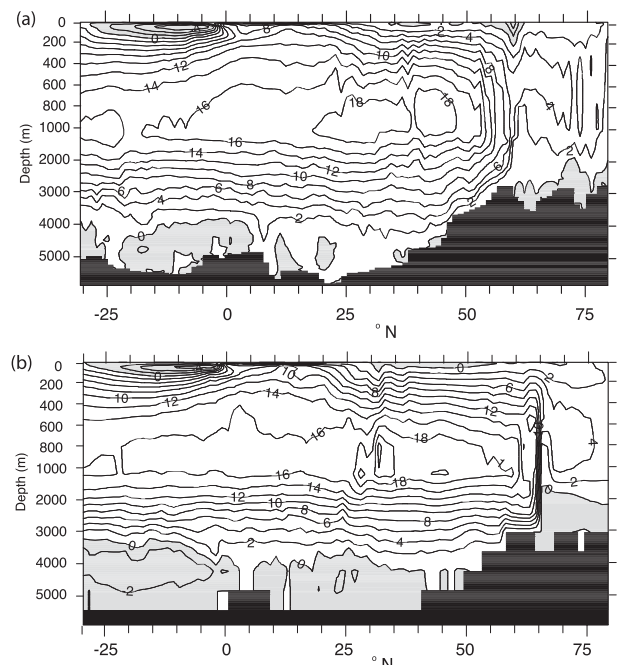


FIG. 6. The meridional overturning streamfunctions (Sv) in the Atlantic domain in years 80–119 of (a) CHIME and (b) HadCM3. Light gray shading indicates regions with negative streamfunction values.

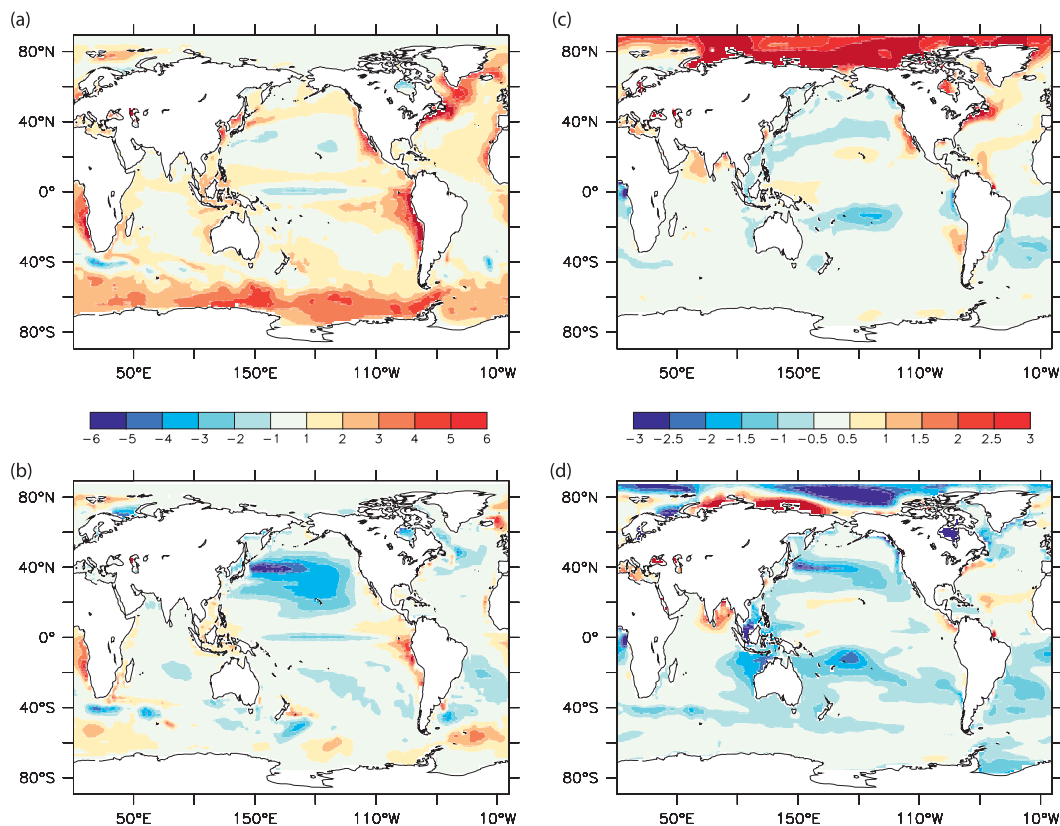


FIG. 7. Ocean surface temperature anomalies ( $^{\circ}\text{C}$ ) from the annual mean NOCS (1999) climatology, averaged over years 80–119 of (a) CHIME and (b) HadCM3, and surface salinity anomalies (PSU) from the annual mean Levitus et al. (1998) climatology in (c) CHIME and (d) HadCM3.

contour is at about 2600 m at  $25^{\circ}\text{N}$  in CHIME and at about 2300 m at the equator, while in HadCM3 the respective depths are 2200 m and about 2100 m. Over 60% of the downwelling in the subpolar gyre in HadCM3 occurs close to the sill region at  $65^{\circ}\text{N}$ , while in CHIME it is spread out over almost  $10^{\circ}$  of latitude. This difference is due mainly to the deeper mixing in the gyre interior in CHIME, but also to reduced mixing in the Labrador Sea in HadCM3 (discussed in section 4c). It is also evident that bottom water formation occurs in the Nordic seas as far as  $75^{\circ}\text{N}$  in both models.

The deep Antarctic Bottom Water (AABW) cell (the reverse cell below 4000 m) is weaker in CHIME, barely reaching  $-1$  Sv in the South Atlantic, compared with stronger than  $-4$  Sv in HadCM3. This is associated with a spindown of the Antarctic Circumpolar Current (ACC; discussed in section 4c), and appears to be due to insufficient production of dense water off Antarctica. As mentioned above, the annual range of ice cover in CHIME is around 40% greater than in HadCM3, so that wintertime heat loss will be reduced, because of the insulating effect of sea ice, and less dense water is produced. It was indeed found that reducing the winter ice cover by doubling the

Southern Hemisphere basal heat flux diffusivity eddydiffs in the ice model produced significant increases in the ACC transport, with an increase of 10–15 Sv relative to the original run after 20 years of reduced ice cover. In addition, an enhanced AABW overturning cell of 3–4 Sv was maintained, similar in magnitude to that in HadCM3 at the same stage of the run. A further improvement of similar magnitude was seen when the piecewise linear vertical regridding scheme in HYCOM was replaced with a higher-order (nonoscillatory piecewise parabolic) scheme.

#### 4. Ocean surface fields and mixed layer depth

##### a. Surface temperature and salinity errors

Figures 7a,b show ocean surface temperature anomalies relative to the annual-mean National Oceanographic Centre, Southampton (NOCS) climatology (Josey et al. 1998), averaged over years 80–119 of CHIME and HadCM3. We shall refer here to model differences from climatology as errors, as do G2000, even though (as has been already remarked) the ocean model is not forced by a present-day atmosphere. This figure corresponds to

Fig. 6a of G2000; in the latter paper the comparison was with the GISST climatology, but the differences relative to the NOCS dataset are very similar. As described in G2000, the surface temperature across most of the global ocean in HadCM3 is remarkably stable over centennial time scales with both the spatial distribution and the magnitude of the differences from climatology remaining almost unaltered over three centuries. The global mean surface error in years 80 to 119 is less than  $0.5^{\circ}\text{C}$ , but there are several regions of significant error: a large cold error of up to  $4^{\circ}\text{C}$  in the North Pacific, a similar cold bias of  $1^{\circ}\text{--}2^{\circ}\text{C}$  over most of the subtropical North Atlantic, warm errors at the eastern boundaries of the Atlantic and Pacific ascribed by G2000 to inaccurate parameterization of marine stratocumulus cloud in the atmospheric model, a warm error of  $1^{\circ}\text{--}3^{\circ}\text{C}$  south of  $50^{\circ}\text{S}$ , and a cold bias of about  $2^{\circ}\text{C}$  along the equator in the central Pacific. Apart from the Southern Ocean and these areas near the eastern boundaries, the surface waters in HadCM3 are generally biased cold. The tendency toward a surface cold bias on the equator is seen in many models of  $1^{\circ}$  or lower resolution (see, e.g., Stockdale et al. 1993), although G2000 ascribe it in HadCM3 to excessive easterly wind stress. The largest coherent SST error in HadCM3, namely the cooling of  $2^{\circ}\text{--}4^{\circ}\text{C}$  across the whole of the subtropical North Pacific, may be clearly seen in Fig. 7b, with the maximum error of  $4^{\circ}\text{C}$  situated around the Kuroshio separation region east of Japan. This error appears rapidly over the whole subtropical gyre during the first decade and is thereafter remarkably stable. No definite explanation for this is proposed in G2000, although they suggest unrealistic heat fluxes in this region, as well as the Kuroshio separation latitude, which is too far south in HadCM3.

In CHIME (Fig. 7a), the warm errors resulting from the unrealistically low cloud cover already mentioned in G2000, particularly off the western coasts of South America and South Africa, are similar to those seen in HadCM3. Since this is a known shortcoming in the atmospheric component common to both models, it is not surprising that the errors are similar in the two coupled models. There is also a significant cold bias of up to  $1.5^{\circ}\text{C}$  in the equatorial Pacific in CHIME similar to that observed in HadCM3. The pattern of SST errors south of the Cape of Good Hope is very similar to that in HadCM3, confirming the suggestion in G2000 that it is due to the low resolution of the ocean model. There is, however, no large-scale SST bias in CHIME in the North Pacific, and instead there is a moderate cold error of  $0^{\circ}\text{--}1^{\circ}\text{C}$  south of  $30^{\circ}\text{N}$  and a warm error of similar magnitude in the subpolar gyre. It is pertinent that subsequent coupled implementations of the Hadley Centre ocean model code, namely HadGEM1 (Johns et al. 2006) and HiGEM

(Shaffrey et al. 2009) both show similar North Pacific cold biases, which strongly suggests that it arises from some—as yet unknown—aspect of the dynamics or physics of this model. CHIME and HadCM3 both have large-scale surface temperature errors across most of the North Atlantic; the errors are warm in CHIME and cool in HadCM3.

CHIME is generally too warm throughout the Southern Ocean, with errors of up to  $3^{\circ}\text{C}$ . This is at least partially due to the use of the KPP mixing scheme in this model, which has been shown to produce unrealistically shallow summer mixed layers in the Southern Ocean in HadCM3 (C. Gordon 2005, personal communication), leading in turn to warm errors of this size in the Southern Ocean; the present version of HadCM3, which uses a bulk mixed layer, still has a warm bias south of  $50^{\circ}\text{S}$ . The SST error in the Southern Ocean in CHIME is highly seasonal, and while the summertime warm error may be over  $6^{\circ}\text{C}$ , in the winter there are many areas colder than the climatology. In the North Atlantic in HadCM3, the surface is  $2^{\circ}\text{--}3^{\circ}\text{C}$  warmer than the climatology off the New England coast, but cooler elsewhere, with a maximum error of  $-5^{\circ}$  at  $48^{\circ}\text{N}$ ,  $53^{\circ}\text{W}$ . In CHIME, the whole subpolar gyre is significantly warmer than climatology, with errors of  $6^{\circ}\text{C}$  centered at  $50^{\circ}\text{N}$ ,  $45^{\circ}\text{W}$ . The cold error in HadCM3 may quite easily be explained by a North Atlantic Current that lies too far to the south; similarly, the warm error in CHIME is consistent with a northwestward displacement of the NAC at  $45^{\circ}\text{N}$  (discussed later), although this cannot entirely explain the warming in the west of the subpolar gyre and the Labrador Sea. Excluding the Southern Ocean and the regions affected by shortcomings in the cloud scheme, the overall impression, however, is that the CHIME SST has a warm surface bias, whereas the HadCM3 has a cold bias (as is the case for other similar level models of the Hadley Centre family). The differences are in addition much larger than those resulting from parameter changes in the HadCM3 model (C. Gordon 2008, personal communication). This further indicates a buildup of heat near the surface in CHIME relative to that in HadCM3, again indicating the possibility of lower mixing in the former.

The different surface temperature errors in the two models would be expected to lead to differences in the atmospheric circulation. The combination of the cold midlatitude bias in HadCM3 and the corresponding warm bias in CHIME mean that the temperature gradient between the equator and the subtropics will tend to be enhanced in the former and reduced in the latter. Examination of the sea level pressure field (not shown) shows broadly rather similar atmospheric circulation in the two models, but the westerlies and trade winds are indeed weaker in CHIME in the North Pacific, with the Aleutian low and North Pacific high both intensified in

HadCM3 compared with CHIME. There is also a northward displacement of the ITCZ in CHIME relative to that in HadCM3, which leads to an increase in rainfall between 10° and 20°N, and a decrease on the equator, relative to that in HadCM3. The surface air temperature (SAT) in CHIME (not shown) is warmer almost everywhere, but particularly so in the Arctic and Antarctic in winter; the global mean SAT in CHIME is about 1°C warmer than that in the NOCS climatology, while in HadCM3 it is about 0.2° cooler.

Figures 7c,d show the surface salinity errors in the two models, relative to the Levitus et al. (1998) climatology. The global surface freshening in HadCM3, described in section 3a, is evident in the dominance of negative (blue shading) anomalies in Fig. 7d, while the mean error in CHIME is rather smaller. However, there are many local similarities. For example, the tripolar error pattern in the Pacific, with the surface being too fresh north of 30°N, too salty between the equator and 30°N and in the Western Warm Pool on the equator west of 180°, and too fresh in the Southern Hemisphere, is of similar distribution and magnitude in both CHIME and HadCM3. Both models are too fresh in the South Atlantic and too salty in the subtropical North Atlantic. A large difference between the models can be seen in the subpolar North Atlantic where HadCM3 is generally too fresh, with a peak error of almost  $-1$  psu centered at 40°W, 50°N, CHIME is over 1 psu too salty over the whole gyre. The fresh anomaly in the Pacific between the date line and 160°W at around 15°S is associated with excessive precipitation in both models (not shown), which indicates an enhanced southern branch of the ITCZ. The surface salinity in CHIME is too high over the whole Arctic, with an error of over 1 psu nearly everywhere, while HadCM3 is too fresh in the central region, but too salty along the Canadian and Eurasian landmasses. However, looking at regional changes in the depth-averaged salinity over the Arctic shows a different picture: the mean salinity in both CHIME and HadCM3 decreases slightly over the first 80 years—by 0.14 psu in CHIME, and by 0.19 psu in HadCM3. The reason for the rather different surface signature is that, where in HadCM3 the relatively warm, salty Atlantic water tongue mixes downward as it moves northward in the Nordic Sea, in CHIME the Atlantic water mixes with the overlying surface freshwater, eroding the shallow halocline; this will be further discussed below.

### *b. Ocean surface circulation and wind stress*

As mentioned in G2000, the large-scale structure of the wind stress field in HadCM3 is generally in good agreement with observations; the same is true of that in CHIME. Differences in the wind stress field between the two models are generally smaller than between either of

the models and the climatology; for the sake of brevity, we will not discuss differences between the models in detail, except in the context of western boundary current separation. In both models the mean wind stress is substantially weaker in the North Atlantic than in the NOCS climatology (Josey et al. 1998), with a maximum eastward stress at 40°W of around  $0.06 \text{ N m}^{-2}$ , as compared with  $0.10 \text{ N m}^{-2}$  in the climatology, and this is likely to influence the strength and path of the ocean circulation. Figure 8 shows the surface velocities of the two models in the North Atlantic, averaged over years 80–119, along with the position of the zero wind stress curl line (ZWCL). Differences in the position of the ZWCL off the eastern seaboard of the United States are clearly visible at about 37°N at 70°W in CHIME and 31°N in HadCM3, while the position of the observed ZWCL (estimated from the NOCS climatology) at this longitude is at 33°N. In CHIME, the Gulf Stream, identified here as the 22° isotherm, separates at about 39°N, while in HadCM3 the separation occurs at around 36°N, close to the observed separation at Cape Hatteras; the more northerly separation of the Gulf Stream in CHIME is therefore broadly consistent with the difference in position of the ZWCL between the two models. The maximum surface speeds in CHIME are significantly stronger than in HadCM3; in the latter, the flow is rather broader and deeper, but despite this the transport of the separated Gulf Stream at 65°W is larger in HadCM3 at around 23 Sv, compared with 15 Sv in CHIME. It should be noted that the Gulf Stream transport in both of these low-resolution models is considerably less than the 80 Sv or so observed at this longitude (e.g., Johns et al. 1995). Comparison of the SST contours in Fig. 8 shows that at 40°W the NAC lies farther north in CHIME than in HadCM3, consistent with the warm SST error in the former and cold error in the latter discussed in section 4a.

G2000 remark that in the North Pacific the zero wind stress curl line in HadCM3 lies farther south than that seen in an atmosphere-only model forced with observed surface temperatures, and that this shift is consistent with the SST error in the ocean component. It is difficult to relate the wind stress curl at the western boundary to the separation position of the Kuroshio, as in the analysis by Hurlburt et al. (1996) of high-resolution simulations, since there is no single clear zero-curl line cutting the western boundary in either of the models or in the climatology. In Fig. 9, we show the time-averaged surface velocities in the northwest subtropical Pacific in the two simulations. The overall features of the circulation are similar in the two models, although there are several significant differences. As in the North Atlantic, both the zero curl and separation of the western boundary current are farther north in CHIME than in observations, while in

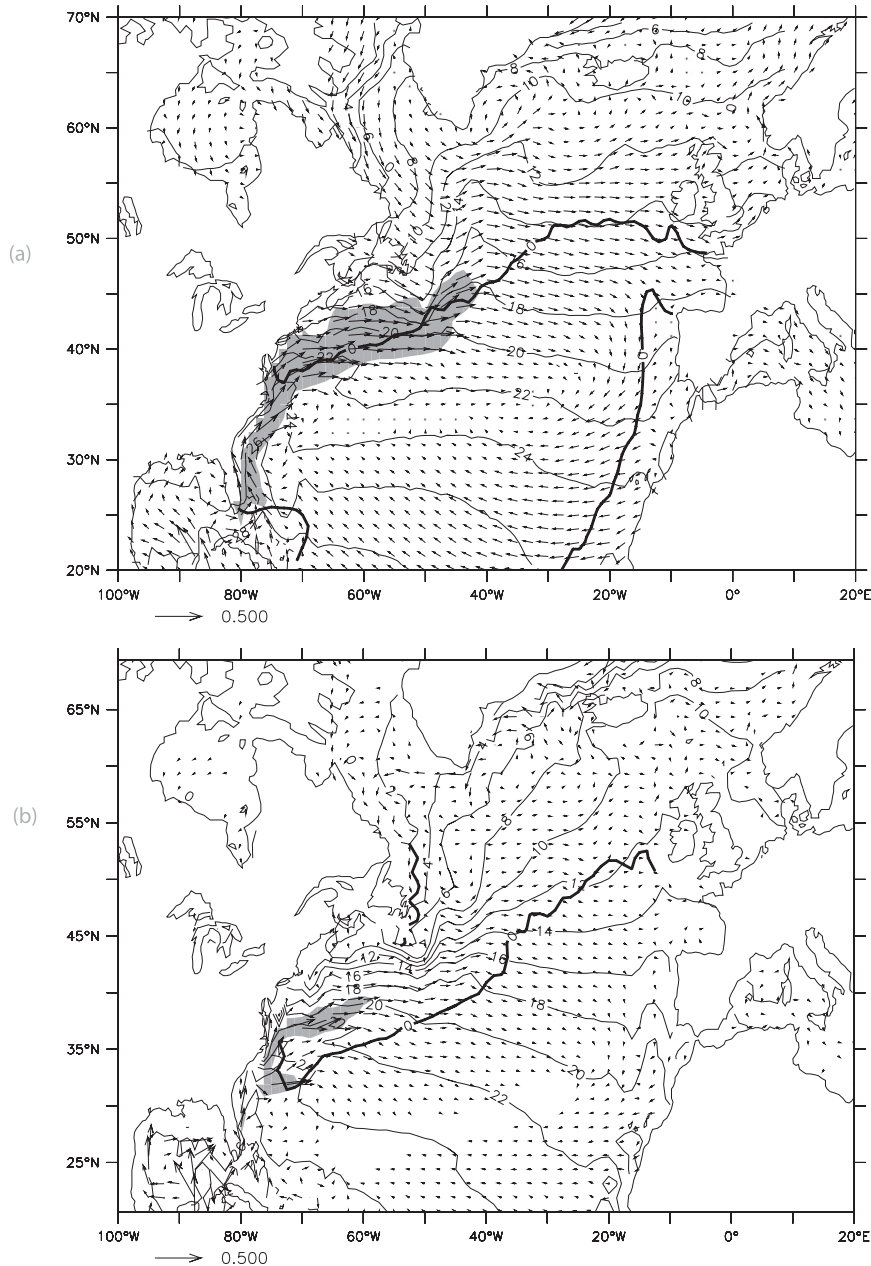


FIG. 8. Surface velocities of (a) CHIME and (b) HadCM3 in the North Atlantic, averaged over years 80–119. The contours show surface temperature errors ( $^{\circ}\text{C}$ ), the solid lines show the position of the mean zero wind-stress curl, and the gray shading indicates speeds  $>0.15 \text{ m s}^{-2}$ .

HadCM3 both are farther south than observed; in the former, the Kuroshio separates at  $37^{\circ}$ – $40^{\circ}\text{N}$ , while in HadCM3 this occurs at around  $31^{\circ}\text{N}$ . In the real ocean, the Kuroshio separates from the coast of Japan at around  $35^{\circ}\text{N}$  (e.g., Qu et al. 2001), and then drifts slightly north of due east, so that by  $180^{\circ}$  the current is centered at about  $38^{\circ}\text{N}$ ; the separation in CHIME is therefore  $3^{\circ}$ – $4^{\circ}$  too far to the north, and in HadCM3 is shifted by a similar distance south. In CHIME, the almost-zonal NPC is centered

at about  $40^{\circ}\text{N}$  when it reaches the date line, while in HadCM3, the core of the NPC is at  $34^{\circ}$ – $36^{\circ}\text{N}$ . Since the surface temperature gradient across these currents is high in the models (a little under  $1^{\circ}\text{C}$  per degree latitude at  $180^{\circ}$ ), the errors of two or three grid points that we have seen in the surface velocity field would be associated with temperature errors of several degrees. Indeed, the surface temperature errors over the whole of the North Pacific in HadCM3 are quantitatively consistent with a southward

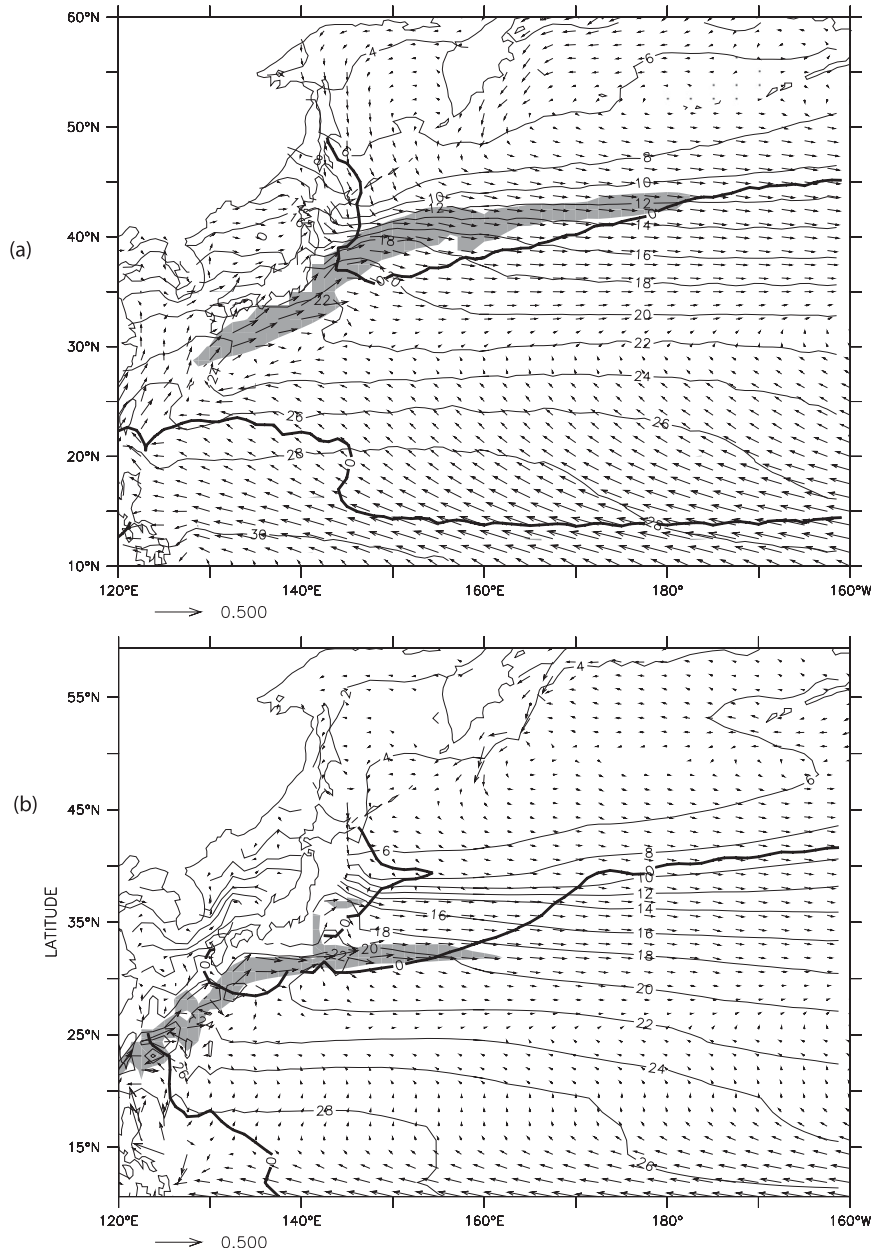


FIG. 9. As in Fig. 8, but for the North Pacific.

displacement of the NPC front by  $3^\circ$  or  $4^\circ$  latitude. It is however difficult to relate the smaller and approximately dipolar SST error in CHIME to the northward displacement of the NPC alone.

The Drake Passage transport in CHIME has a realistic value of 140 Sv in the first decade, but spins down to 60 Sv by year 200; in HadCM3, by contrast, the transport increases gradually for the first 150 years, reaching 200 Sv by year 100, significantly higher than the observed transport of around 135 Sv (Cunningham et al. 2003). In

CHIME the spindown is associated with a gradual warming of the deep waters around Antarctica, as discussed in section 3c, which leads to a slumping of the isopycnals at the frontal region at the ACC (although the disappearance of dense layers in the Southern Ocean seen in some isopycnal models is not seen in CHIME). It should be noted that the vigorous ACC seen in HadCM3 is not necessarily representative of all  $z$ -coordinate ocean models (several of the models published in the IPCC Third and Fourth Assessment Reports have lower ACC transports than that

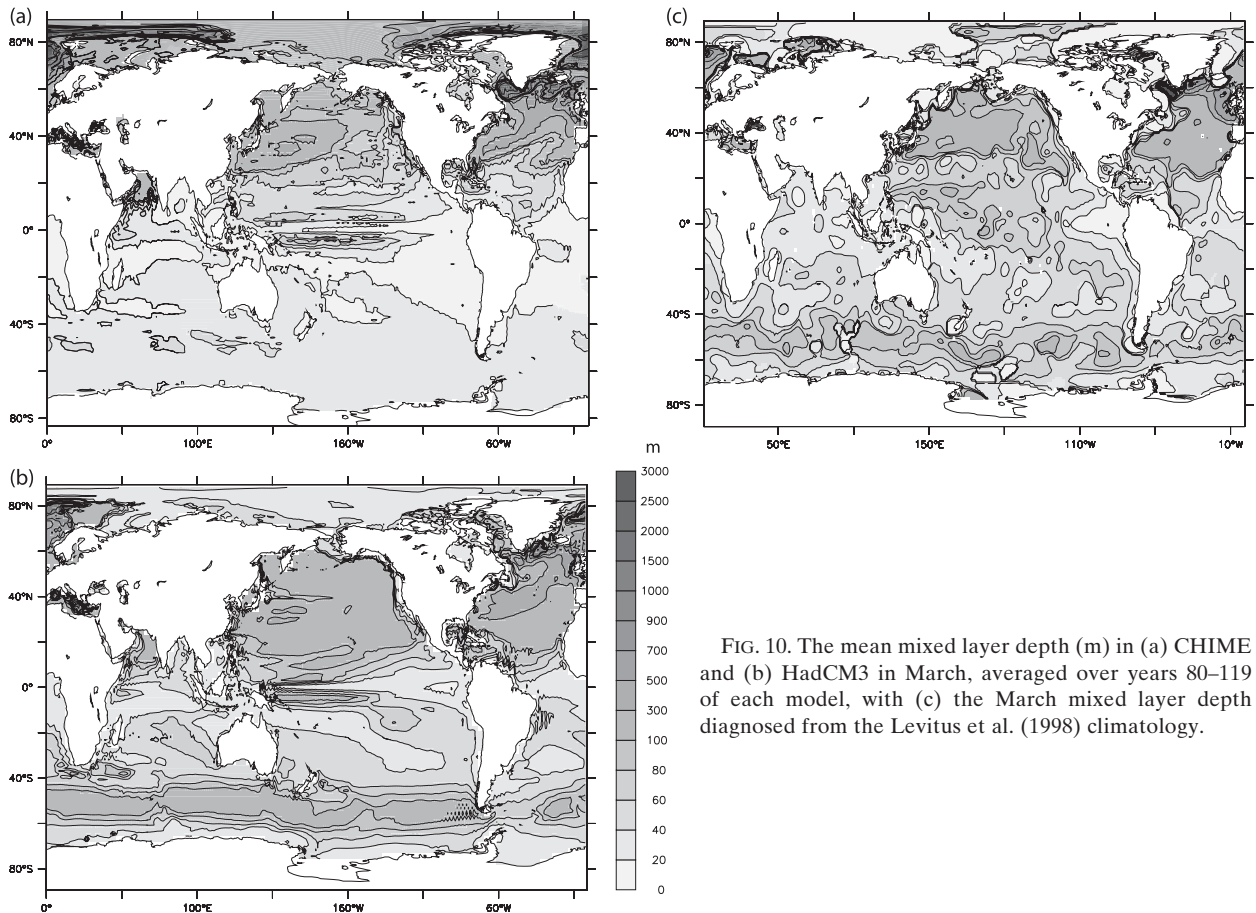


FIG. 10. The mean mixed layer depth (m) in (a) CHIME and (b) HadCM3 in March, averaged over years 80–119 of each model, with (c) the March mixed layer depth diagnosed from the Levitus et al. (1998) climatology.

observed), but the difference in the present comparison is striking, given the identical atmosphere component.

As we noted in the introduction, the more realistic coastlines in CHIME allow the Bering Strait and Canadian Archipelago to be modeled explicitly. The flow through the Bering Strait into the Arctic is rather variable, lying between 0 and +1 Sv, compared with an observed barotropic flow of around 0.8 Sv (Roach et al. 1995). The flow through the Canadian Archipelago is southward, with a transport of about 2 Sv through Davis Strait, which is in good agreement with observations (e.g., Cuny et al. 2005). We note that the southward export of dense water with  $\sigma_2 > 37.6$  through the Denmark Strait into the North Atlantic in CHIME is about 3 Sv, with an additional southward flow of about 3 Sv of dense water over the Iceland–Scotland ridge system; this is in broad agreement with observations.

### c. Mixed layer depth

In this section we compare the mixed layer depth (MLD) in the models with that in the Levitus et al. (1998)

climatology. The MLD fields shown here from HadCM3 and from the Levitus dataset have been recalculated from the monthly mean temperature and salinity according to a density change equivalent to a temperature difference of 0.5°C, to enable a more meaningful comparison with the MLDs thus diagnosed in CHIME. Figure 10 shows the mean MLD in HadCM3 and CHIME in March, averaged over years 80–119 of each model, alongside the March mixed layer depth derived from the Levitus climatology; March was chosen to show the winter convection in the Northern Hemisphere, at the same time as revealing summer biases in the Southern Ocean. The shallow bias in the Southern Hemisphere summer in CHIME is immediately obvious; the MLD is nowhere deeper than 50 m across the whole Southern Ocean, where in the climatologies and in HadCM3 there is a band of mixing to around 100 m between 40° and 60°S spanning the whole circumpolar region. This overly shallow MLD in the austral summer is the principal reason for the SST being too warm in CHIME in this region. In the Northern Hemisphere, the overall pattern of winter mixing in the two models is similar to that in Levitus, although there

are regional differences. In the North Pacific both models reproduce the tongue of mixing to 300–400 m in the Kuroshio separation region, as well as the 100–200-m depth of the wintertime mixed layer north of 20°N, although elsewhere in the North Pacific the mixed layer depth in HadCM3 is too deep, possibly because of the depressed surface temperature. In the North Atlantic the mode-water formation region extending northeastward from the Sargasso Sea to 30°W is well represented by both models, with realistic MLDs of 300–450 m. The pattern of deep convection from the Labrador Sea in the west, to northwest of Scotland in the east, is clear in both models; the mixing is deeper in CHIME than in Levitus, penetrating to 1500 m south of the whole sill system and below 2000 m in the Labrador Sea, while in HadCM3 the mixing is similar to that estimated from the climatology, although there is little mixing in the Labrador Sea. The mixing in the Nordic Sea in HadCM3 is realistic, but in CHIME the convection is too deep (up to 4000 m) and extends not only across most of the Nordic Sea but through Fram Strait and as far as the Canadian Basin. This excessive mixing is consistent with the anomalously high surface salinity, and the resulting decrease in stratification, that develops in CHIME in the North Atlantic subtropical gyre and the Arctic.

## 5. Interior water mass preservation

### *a. Thermocline evolution in the subtropical gyres*

The ocean component of HadCM3 uses the Gent and McWilliams (1989) formulation for isopycnal diffusion, which reduces the diapycnal component of the explicit horizontal diffusion. This scheme was shown by Danabasoglu and McWilliams (1995) to lead to a sharper thermocline than in the case when only horizontal diffusion is used. We will show in this section that the ocean component of HadCM3 nevertheless shows significant broadening of the thermocline in the subtropical gyres, which is not seen in the hybrid ocean of CHIME. Figure 11 shows the temperature drift in the subtropical regions (here defined to lie between 10° and 48°N, and between 10° and 30°S) for CHIME and HadCM3. Comparison with Figs. 3a,b confirms that the global temperature drift described earlier in both models is to a large extent consistent with the changes in the subtropical gyres. This is especially true in CHIME, where both the pattern of warming above 500 m and cooling between 500 and 1500 m and the magnitude of the changes are very similar in the global and subtropical means. In HadCM3 the cooling of the upper 200 m in the subtropical gyres is offset in the global mean by surface warming in the Southern Ocean and Arctic, but below 300 m the pattern

of warming in the subtropical gyres is rather similar to that in the global average.

Figure 12 shows the time evolution of the mean temperature in the subtropical North Atlantic between 10° and 48°N as a function of depth, in CHIME and HadCM3. As described in section 5a, both models warm at depth, although rather less in CHIME than in HadCM3. It is also clear that CHIME preserves the initial strong stratification between 400 and 800 m more faithfully than does HadCM3; in the latter, the temperature contours diverge over 200 years, with significant warming beneath the thermocline consistent with enhanced vertical diffusion. In the subtropical gyre in the North Pacific (not shown) there is a similar downward migration of the isotherms at the base of the thermocline in HadCM3, while in CHIME the thermocline structure is unchanged after 200 years.

We have shown that the global drifts of temperature and salinity in CHIME are consistent with a reduced mixing in the depth range between 300 and 800 m compared with that in HadCM3 and that this process occurs most coherently in the subtropical regions. The question then arises as to whether the diffusion in the tropical thermoclines in CHIME might be too weak, since Fig. 12a shows that the temperature gradient in the depth range 400–600 m increases during the 200-year run, relative to an initial state, which is based on climatology. In Fig. 13 we show temperature contours at 25°N for both models, along with observations from a section carried out at this latitude (Cunningham 2005). It is clear that both models underestimate the east–west slope in the basin interior, which is consistent with the low wind stress already mentioned. West of 60°W, both models represent the separation of the 14° and 20°C isotherms realistically, even though the thermocline in HadCM3 is evidently not well resolved by the level spacing, but east of that longitude the mean stratification in CHIME is much closer to that in the observations. We therefore conclude that the subtropical thermocline is well represented in CHIME, and that at least the initial drift is caused by adjustment from the oversmoothed climatology used to initialize the ocean model.

### *b. Antarctic Intermediate Water and Subantarctic Mode Water*

Antarctic Intermediate Water (AAIW) is formed through surface mixing around the Southern Ocean between 45° and 55°S, is subsequently subducted and spreads northward almost adiabatically (Talley 1996), and is characterized by a subsurface salinity minimum. Figure 14 shows salinity sections at 30°W in the initial states and at 80 years of CHIME and HadCM3. At initialization, a salinity minimum is clearly visible between

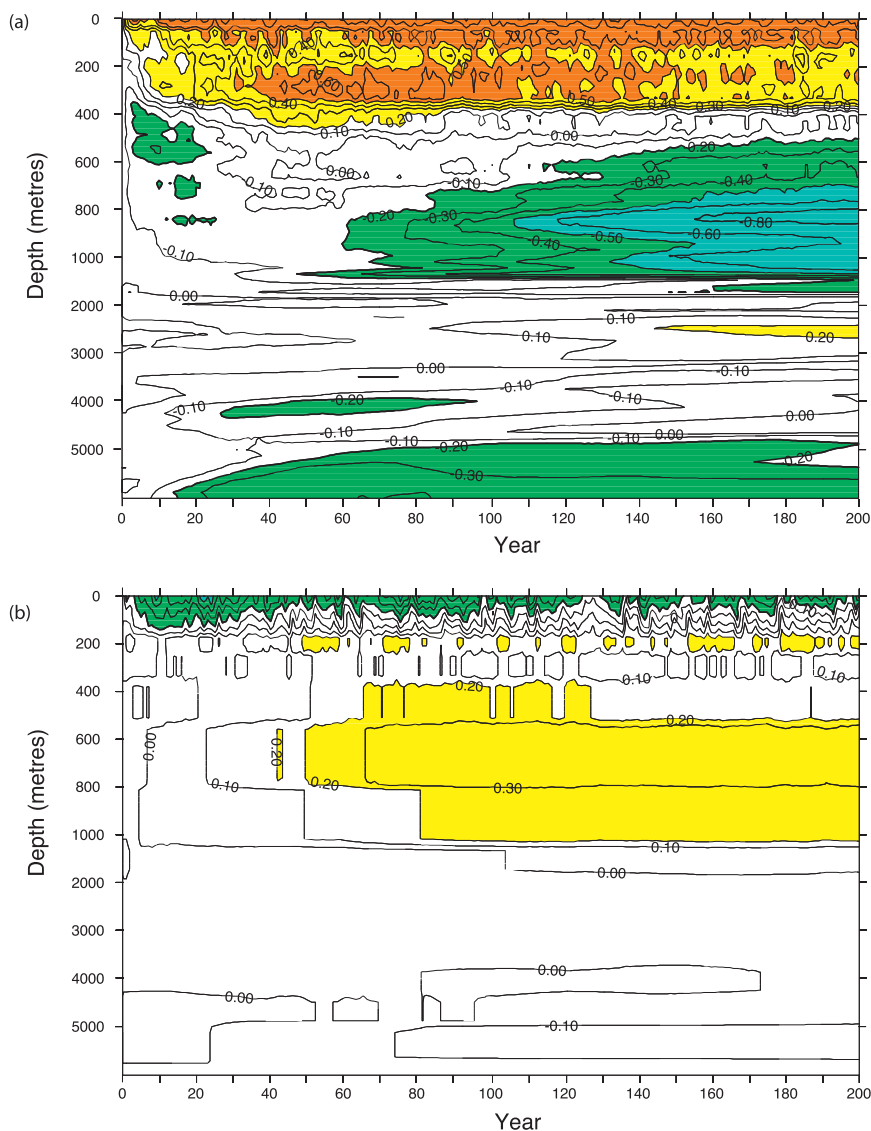


FIG. 11. The temperature drift ( $^{\circ}\text{C}$ ) in the subtropical regions (here defined to lie between  $10^{\circ}$  and  $48^{\circ}\text{N}$ , and between  $10^{\circ}$  and  $30^{\circ}\text{S}$ ) in (a) CHIME and (b) HadCM3.

$50^{\circ}$  and  $10^{\circ}\text{S}$  in both models. In CHIME, a low salinity of 34.50 psu is clearly maintained as far as  $12^{\circ}\text{S}$ , although the volume of AAIW is reduced, and the core rises from 1000 m at initialization to around 600 m by year 80. In HadCM3, by contrast, after 80 years the salinity minimum is hardly discernable north of  $20^{\circ}\text{S}$ . In addition, Fig. 14 also shows a progressive freshening in CHIME south of  $45^{\circ}\text{S}$ , so reducing the density contrast across the ACC, while HadCM3 maintains the north–south density difference and hence the strong ACC described above. Overall, the fresh signature of AAIW is better maintained in CHIME than in HadCM3. The ability of HYCOM to preserve water mass characteristics is similarly evident (not shown here) in the North Pacific, where the fresh

tongue of North Pacific Intermediate Water is maintained with little variation over the 200-yr run of CHIME, but is significantly eroded after a few decades in HadCM3.

Subantarctic Mode Water (SAMW) is formed along the northern side of the Antarctic Circumpolar Current, and in the real ocean has a characteristic biogeochemical signature with a low ratio of silicate to nitrate. This allows SAMW to be traced widely around the global ocean, and also has implications for the balance of species in marine ecosystems (Sarmiento et al. 2004). It is therefore important for numerical models that include ecosystem models for the properties of SAMW to be preserved in a realistic way during its dispersal away from its source region. SAMW also has a clear minimum in stratification

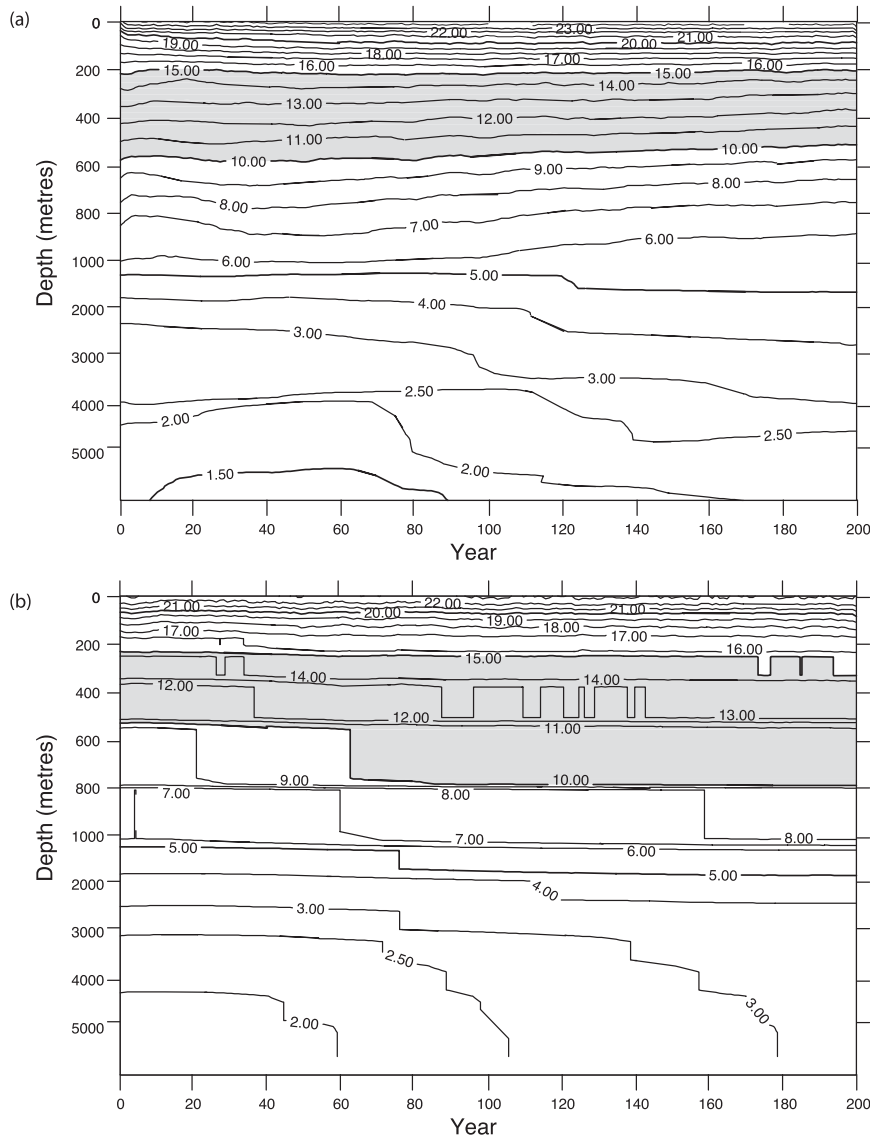


FIG. 12. The time evolution of the mean temperature ( $^{\circ}\text{C}$ ) in the subtropical North Atlantic in (a) CHIME and (b) HadCM3 as a function of depth. Regions with temperatures between  $10^{\circ}$  and  $15^{\circ}\text{C}$  are shaded.

and hence potential vorticity (PV), which is again traceable for thousands of kilometers. Banks et al. (2002) show that in HadCM3, the formation of SAMW is particularly sensitive to climate change, and is a highly efficient conduit for the uptake of heat by the ocean. This implies that for this heat to be redistributed correctly within the ocean, the dispersal of SAMW should be associated with a realistic diffusion without excessive spurious numerical mixing. Sloyan and Kamenkovich (2007) examine the representation of SAMW in a suite of climate models with  $z$ -coordinate oceans (including HadCM3), and conclude that all of the models are overdifusive, underestimating the density at the potential vorticity minimum

and only showing limited northward extension of the PV minimum. SAMW may be identified all around the Southern Ocean, and in the salinity sections at  $30^{\circ}\text{W}$  shown in Fig. 14, SAMW may be seen immediately as the region of intermediate salinity in the range between 34.70 and 35.30 psu above the fresh AAIW tongue between  $45^{\circ}$  and  $20^{\circ}\text{S}$ . A large fraction of SAMW production occurs in the southeast Indian Ocean, and in Fig. 15 we show the potential vorticity on a north–south section in the central Indian Ocean at initialization and after 80 yr in CHIME and HadCM3. In the initial state of CHIME (Fig. 15a), SAMW is the body of water in the depth range between 150 and 800 m and between  $43^{\circ}$  and  $30^{\circ}\text{S}$ ,

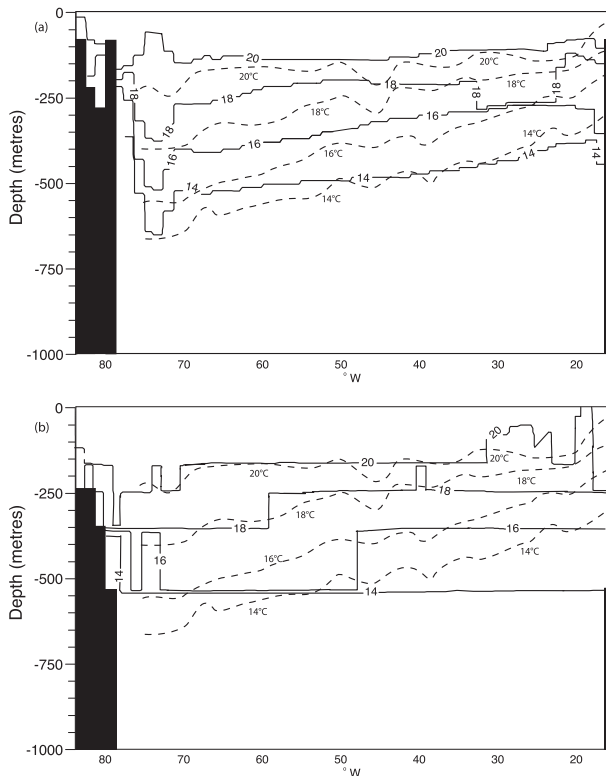


FIG. 13. Temperature contours ( $^{\circ}\text{C}$ ) (solid lines) at  $24^{\circ}\text{N}$  in April of year 80 of (a) CHIME and (b) HadCM3, with the dotted lines showing isotherms as observed by Cunningham (2005).

identified with a clear local minimum in magnitude of PV with values between  $-4$  and  $-10 \times 10^{-11} \text{ m}^{-1} \text{ s}^{-1}$ , and the northward path of the subducted SAMW is also visible, extending north from  $20^{\circ}\text{S}$ . After 80 years, the low stratification in the formation region is well preserved in CHIME, as is the subduction route; in fact the stratification above and below the SAMW increases. In HadCM3, by contrast, the salinity contrast between the SAMW and the underlying AAIW is clearly eroded at  $30^{\circ}\text{W}$ , and the region of low stratification between  $43^{\circ}$  and  $35^{\circ}\text{S}$  in the initial state is no longer visible, while there is no sign of the subducted SAMW north of  $20^{\circ}\text{S}$ .

### c. North Atlantic Deep Water and Bottom Water structure

We have shown in section 3c that there are differences in the meridional overturning streamfunction between CHIME and HadCM3, with the southward-flowing NADW lying at shallower depths in HadCM3. Examination of Fig. 6 shows that, between  $30^{\circ}$  and  $50^{\circ}\text{N}$ , whereas the  $2\text{-Sv}$  contour in HadCM3 becomes horizontal at a depth of 3600 m, in CHIME the overflow water continues to follow the slope down to a depth of greater than 4000 m, which is consistent with reduced

mixing of the dense overflows in the latter model. Figure 16 shows the temperature averaged over the bottom 50 m in the North Atlantic in the initial states of CHIME and HadCM3, as well as that in year 80 of each model. It can be seen that, at the start of both models, a large body of water colder than  $2.0^{\circ}\text{C}$  lies at the abyss in both sides of the basin, while the bottom temperatures in the Nordic Basin are initially below  $0.5^{\circ}\text{C}$ . After 80 years, CHIME preserves the cold water in the western side of the basin, and indeed south of  $30^{\circ}\text{N}$ , the abyssal water has cooled slightly to  $1.0^{\circ}\text{--}1.5^{\circ}\text{C}$ , while, east of the Mid-Atlantic Ridge, a warming of around  $1^{\circ}\text{C}$  is evident. The path of the overflow water is clearly visible as a continuous ribbon of water colder than  $2^{\circ}\text{C}$ , extending through Denmark Strait as far as  $30^{\circ}\text{N}$ , which may indeed be underdiffused relative to observations. Examination of the bottom salinity (not shown) identifies the cold water south of  $30^{\circ}\text{N}$ , east of the Mid-Atlantic Ridge in CHIME as Antarctic Bottom Water, and we ascribe the abyssal warming there to the reduced northward circulation of AABW in that model. In HadCM3, by contrast, the bottom waters west of the Mid-Atlantic Ridge warm by between  $1^{\circ}$  and  $2^{\circ}\text{C}$  by year 80, and the DWBC is not present as a distinct flow, although the cold bottom waters are well preserved in the eastern basin. The improved representation of the abyssal flow in the hybrid ocean model in CHIME, where the thickness of the densest mass-containing layer is limited only by the balance between advection and diffusion, is obvious; in HadCM3, the progressive penetration of heat into the abyss discussed earlier in this section, can be seen here to result in drift farther away from the initial state. This is consistent with the observations of Roberts et al. (1996) in intercomparison studies using ocean-only models, where the dense overflows in the  $z$ -coordinate model mixed rapidly with the overlying water, resulting in warming in the deep ocean.

The vertical structure of NADW is indeed known to be generically poorly represented in  $z$ -coordinate models (Saunders et al. 2008). In Fig. 17 we show the zonally averaged transport per unit depth in the North Atlantic at  $26^{\circ}\text{N}$  in HadCM3 and CHIME, superposed on Fig. 1 from Saunders et al., which shows the same quantity for three relatively high-resolution ocean models, along with estimates from observations. In CHIME, while the AABW cell is weaker than that observed (in fact, none of the models represents the circulation below 4000 m faithfully), the region between 1500 and 4000 m with low vertical shear is well simulated; this is in marked contrast to the maximum in the southward transport seen at 1500–2500 m, which is seen in the other models, and the gradual reduction with depth below this. It is interesting to note that HadGEM1 (Johns et al. 2006), with

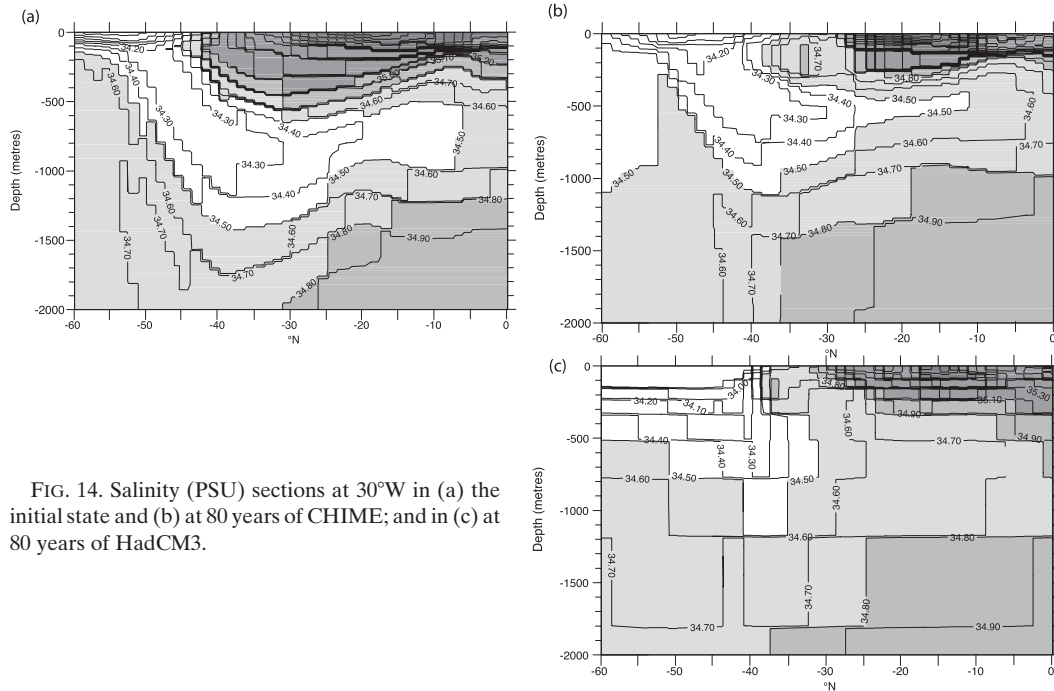


FIG. 14. Salinity (PSU) sections at 30°W in (a) the initial state and (b) at 80 years of CHIME; and in (c) at 80 years of HadCM3.

essentially the same ocean physics as HadCM3, but higher spatial resolution, shows a very similar depth structure of the NADW flow. In the context of long-time-scale climate simulation, this may be regarded as a key improvement over the shallower NADW in HadCM3.

## 6. Summary and discussion

We have presented results from a new coupled climate model, CHIME, which is based on the Hadley Centre's HadCM3, having the same atmosphere, land, and sea ice

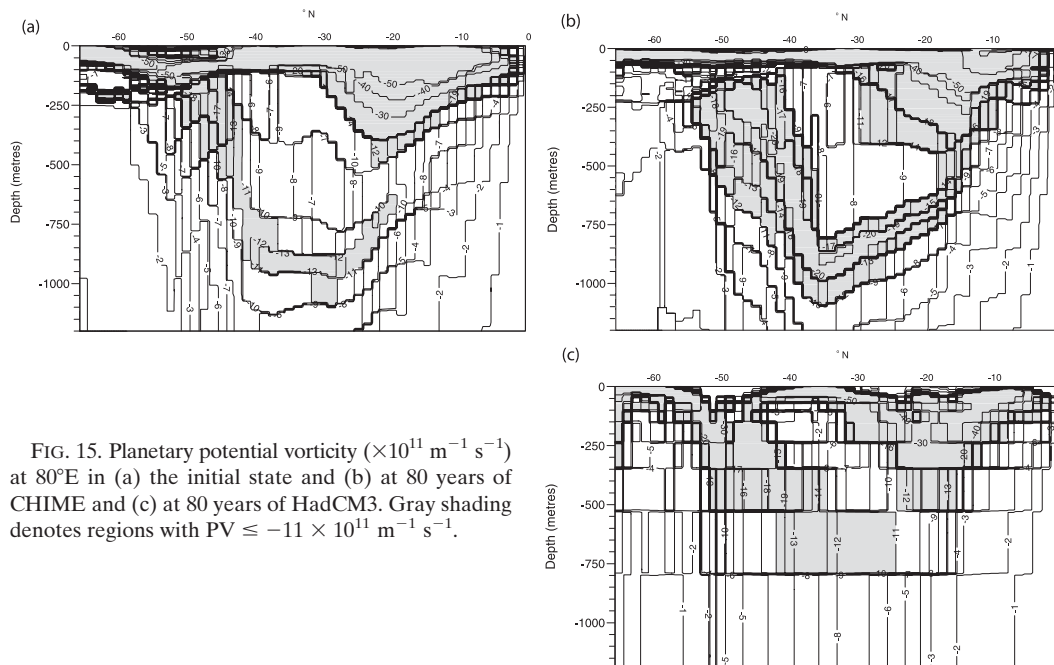


FIG. 15. Planetary potential vorticity ( $\times 10^{11} \text{ m}^{-1} \text{ s}^{-1}$ ) at 80°E in (a) the initial state and (b) at 80 years of CHIME and (c) at 80 years of HadCM3. Gray shading denotes regions with  $\text{PV} \leq -11 \times 10^{11} \text{ m}^{-1} \text{ s}^{-1}$ .

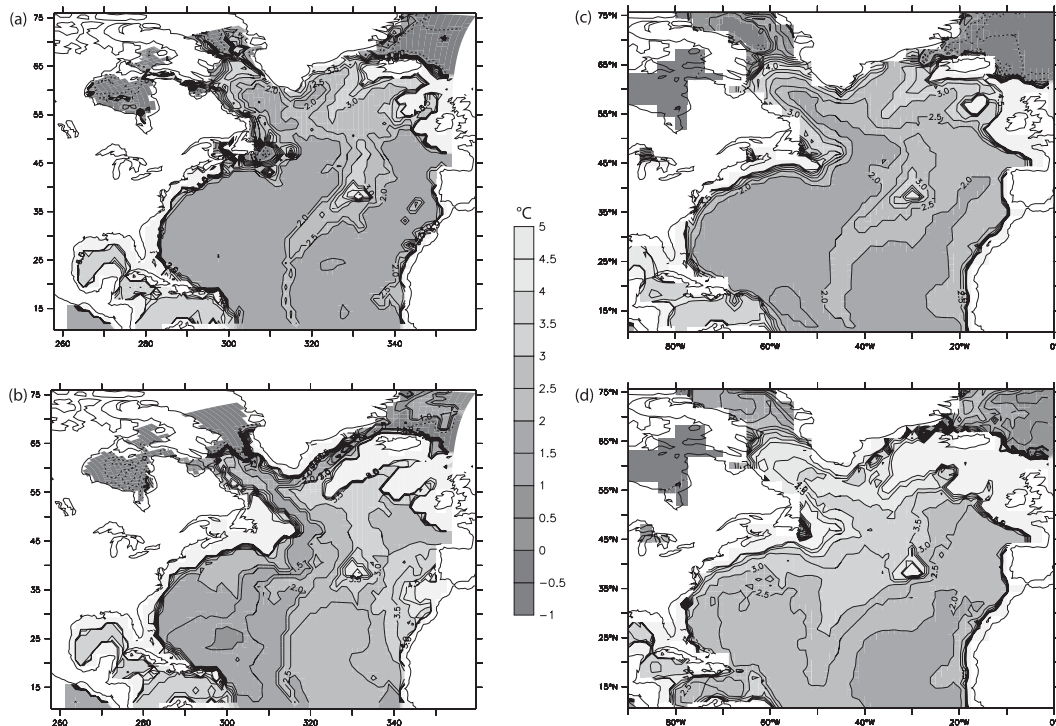


FIG. 16. Bottom temperature ( $^{\circ}\text{C}$ ) in the North Atlantic in (a) the initial state, (b) year 80 of CHIME, (c) the initial state, and (d) year 80 of HadCM3.

models, but uses a hybrid-coordinate ocean component (HYCOM) instead of constant-depth levels. To our knowledge, this is the first comparison in which an existing coupled climate model has been rerun with a structurally different ocean component, with the atmosphere component remaining completely unchanged. CHIME has been run for 200 years with preindustrial atmospheric forcing, and shows a low overall drift after 40 years without the need for flux correction, and we have compared this integration with a similar control integration of HadCM3.

The two models show marked similarities in overturning circulation and heat transports, with a maximum overturning in the North Atlantic of 18–20 Sv in both models, and global northward ocean heat transports within the bounds of observational estimates. Many other features of the models are similar, including the wind stress and the heat and freshwater fluxes, as well as more specific features such as the warm sea surface biases at the eastern coasts, which have been ascribed to errors in the cloud scheme of the HadAM3 atmosphere model. However, striking differences are also evident. In particular, the globally averaged sea surface temperature (SST) is much warmer in CHIME than in HadCM3, while the cold sea surface error in the North Pacific in HadCM3 is absent in CHIME. CHIME has a warm and salty error in the North Atlantic,

where HadCM3 has a smaller cold error associated with a southward deviation of the NAC and a fresh surface error over the whole North Atlantic. The volume transport of the Gulf Stream at  $65^{\circ}\text{W}$  is smaller in CHIME at around 15 Sv, compared with 23 Sv in HadCM3. This difference is larger than that between the heat transports in the two models, and this is qualitatively consistent with the higher thermocline stratification in CHIME.

The Arctic in CHIME has a bias toward high surface salinity, which is due to anomalously strong upward mixing of Atlantic water. This behavior is perhaps surprising, since the hybrid-coordinate model would be expected to preserve vertical gradients, but the upward mixing may be associated with the use of  $\sigma_2$  as the vertical coordinate, in which the density stratification in the upper few hundred meters in the Arctic is significantly reduced compared with that in  $\sigma_{\theta}$ , and possibly with the anomalously high temperature and salinity of the incoming Atlantic water. This error might be partially ameliorated by increasing the ocean resolution in the relevant density range. CHIME also has mixed layer depths that are too shallow in the summer but too deep in the winter, particularly in the Southern Ocean where there is a warm surface bias in the summer as a result. The latter is attributed to the use of the KPP mixing scheme in CHIME, instead of the bulk mixed layer implemented in HadCM3.

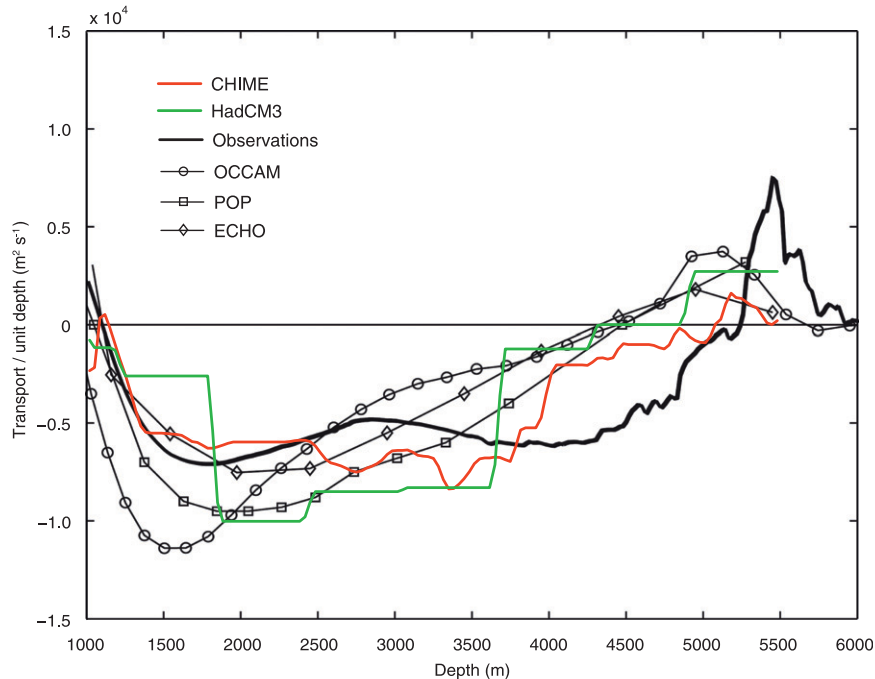


FIG. 17. Transport per unit depth ( $\text{m}^2 \text{s}^{-1}$ ) in the Atlantic at  $25^\circ\text{N}$  in years 80–119 of HadCM3 (green) and CHIME (red). Also shown are the curves from Fig. 1 of Saunders et al. (2008): three high-resolution ocean-only models (diamonds, circles, and squares), while the bold black line shows estimation from observations.

The two models show clear differences in separation position of the western boundary currents in Northern Hemisphere, which are matched by shifts in position of the zero wind stress curl line in both models; in the North Pacific, the Kuroshio separates farther south in HadCM3 and farther north in CHIME than in observations, and in the North Atlantic the models show similar differences in the position of the Gulf Stream separation. The reason for these differences is yet unknown; a prime candidate is the fact that HadCM3 uses a B grid where HYCOM uses a C grid, which would change the way that coastal currents “feel” the coastline. Although the coastlines in CHIME are less blocky and more realistic than in HadCM3, this is unlikely to be the reason for the observed differences in separation position, since similar changes were observed in the AIM, DYNAMO, and GIM ocean-only comparisons, where coastlines were the same in each model of the respective group. Another possible reason for difference in the different separation positions is the differing ability of the ocean components of CHIME and HadCM3 to represent the Deep Western Boundary Current. In HadCM3, the southward displacement of the North Pacific Current is associated with the cold surface error in that model, but it is far from obvious why CHIME, with a similar but opposite displacement of the NPC, does not show a corresponding warm error. The fact that the HadCEM and HadGEM, with higher resolution ocean components than

that of HadCM3, also show cold errors in the North Pacific implies that this feature is not related to model resolution.

We would expect many of the differences between HadCM3 and CHIME to be related to the rate of transfer of surface properties into the ocean interior, and to the degree of preservation of the interior water masses, whereas spurious numerical diapycnal mixing due to the model’s advection scheme would be expected for  $z$ -level models such as HadCM3, the isopycnic formulation of HYCOM is specifically designed to eliminate this process entirely. It is difficult to assess the explicit diffusivities directly in either CHIME or HadCM3, since these were not archived in either of the experiments described here, although the background value used in both cases (around  $1.0 \times 10^{-5} \text{ m}^2 \text{ s}^{-1}$ ) is small. Nevertheless, we have shown evidence that CHIME has significantly less mixing in the upper, intermediate, and deep ocean than does HadCM3; namely, the better preservation of the signatures of Antarctic Intermediate Water and Subantarctic Mode Water in the hybrid-coordinate ocean model; the more realistic vertical structure of the southward-flowing North Atlantic Deep Water in CHIME; the sharper and more realistic thermocline in the subtropical gyres; and the reduced mixing of the dense overflow waters in the North Atlantic. The surface and near-surface warming seen in CHIME is consistent with this improved water mass preservation, as heat at the surface is not diffused downward as quickly as

in HadCM3, whereas the warming drift in HadCM3 penetrates from the near surface down to 800–1000 m by year 60 before stabilizing, the warming in CHIME only reaches to 400 m, and is correspondingly larger, mainly because it is confined to a smaller region. Similarly, sharpening of the main thermocline in CHIME is evidenced by cooling between 500 and 800 m, whereas this region warms in HadCM3. This would seem to imply that by adding extra mixing to CHIME in the main thermocline, the evolution of the globally averaged heating of the upper and intermediate layers of the two models could be made rather more similar. These model differences would be expected to be critical in long-time-scale climate predictions, since the evolution of the ocean state is known to play a crucial role in climate dynamics on time scales of decades and longer; indeed, G2000 describe centennial-time-scale drifts in deep water mass structure and in the overturning circulation in the North Atlantic in HadCM3.

The substantial warming and increasing salinity in the North Atlantic subpolar gyre in CHIME are clearly not realistic, and the reasons for these changes are complex and still not completely understood. Similar internal changes occur in HadCM3, but with a smaller magnitude, and in that model their surface signature is much reduced by a layer of freshwater, with salinity more than 1 psu lower than observed values, in the upper 200 m. There is also a northwestward deviation of the path of the North Atlantic Current in CHIME, which contrasts with the southeastward deviation of the NAC in HadCM3. It has been demonstrated in ocean-only simulations that the path of the North Atlantic Current is more realistic in ocean-only isopycnic models forced by realistic surface fluxes than in comparable  $z$ -coordinate models, so the question arises as to why in this case the isopycnic model has a less realistic gyre circulation in the North Atlantic than does HadCM3. The fact that the wind stress is rather lower in both CHIME and HadCM3 than that observed may well contribute to the difference in NAC path in the two models; with a deficit in the northeastward stress over the NAC, the error in the Ekman transport will at least initially result in a northwestward transport anomaly in the surface layers, which would bring warm, salty water into the subpolar gyre. It is possible that in HadCM3 this will partially be offset by the tendency, observed in ocean-only implementations of this model, for the NAC to lie too far to the south. Finally, it is remarkable that the rather different temperature and salinity anomalies in the upper ocean in the North Atlantic in the two models do not result in large differences in the overturning circulation; HadCM3 maintains an overturning of 20 Sv despite its fresh surface layer (although the deep water formation region does largely migrate to the Nordic seas, where the surface salinity is more realistic), and in CHIME the

overturning remains at a similar value even though there are large-scale changes in the surface temperature and salinity in the region.

While we conclude that there is markedly reduced interior mixing in the CHIME model as compared with HadCM3, it is only right to state that the ocean component of CHIME also has known deficiencies such as lack of vertical resolution in near homogenous regions such as high polar latitudes, and has only an approximate representation of the pressure gradient (which may affect the ability of the model to represent the vertical shear in the water column and hence the northward penetration of Antarctic Bottom Water). In addition, the version of HYCOM used in this experiment has a significant degree of nonconservation of heat and salt, which will have unknown consequences for longer integrations. The present comparison is between just one integration of each model type, and we admit that it is difficult to disentangle the effects of changing the vertical coordinate from those of other differences between the models, such as the different grids, coastlines, and vertical mixing schemes; further sensitivity studies would be required to investigate this. The present exercise is, indeed, not about showing which model is “better” as clearly both models have drawbacks and there is no obvious winner. Nor do we claim that the results presented here for the two models are necessarily representative in any definitive sense of every climate model sharing the respective class of ocean model. Rather we have shown the critical importance of changing just one component of the climate system.

Overall, therefore, this paper begins to address the structural uncertainty in climate models and their projections by examining the differences that arise from such structural changes. While both HadCM3 and CHIME are “good” models from the point of view of their heat transports being within observational estimates, and possessing strong, robust, and remarkably similar overturning circulations, there are clear and marked differences between the two in their representation of the mean climate in control integrations, and it seems that the large part of these differences are caused by differences in interior mixing. Given that the mean ocean climates in these control simulations are very different, we would expect their projections of future climate change also to be different, and possibly that different mechanisms might be involved in driving the evolutions of the models. Differences arising from structural changes to our present suite of climate models therefore need to be properly and fully assessed.

*Acknowledgments.* We acknowledge NERC/SOC Core Strategic, NERC COAPEC funding (Grant NER/T/S/

2001/00187) and the NERC RAPID THCMIP project (Grant NE/C522268/1) for this work. We are grateful to Rainer Bleck and Shan Sun at NASA GISS for their initial contributions to setting up the ocean model, and to Jeff Cole at CGAM, University of Reading, for his assistance in installing the Unified Model. We would also like to thank Chris Gordon, Richard Wood, Helene Banks, and many other colleagues at the Hadley Centre for supplying HadCM3 output data and help in analysis of the coupled model. The authors are grateful to Robert Marsh for his comments on the manuscript, and would like to thank the three anonymous reviewers, whose suggestions significantly improved the paper.

## REFERENCES

- Banks, H., R. Wood, and J. Gregory, 2002: Changes to Indian Ocean Subantarctic Mode Water in a Coupled Climate Model as CO<sub>2</sub> forcing increases. *J. Phys. Oceanogr.*, **32**, 2816–2827.
- Bleck, R., 2002: An oceanic general circulation model framed in hybrid isopycnic-cartesian coordinates. *Ocean Modell.*, **44**, 55–88.
- , and L. T. Smith, 1990: A wind-driven isopycnic coordinate model of the North and Equatorial Atlantic Ocean. 1: Model development and supporting experiments. *J. Geophys. Res.*, **95C**, 3273–3285.
- Cattle, H., and J. Crossley, 1995: Modelling Arctic climate change. *Philos. Trans. Roy. Soc. London*, **352A**, 201–213.
- Chassignet, E. P., L. T. Smith, R. Bleck, and F. O. Bryan, 1996: A model comparison: Numerical simulations of the North and equatorial Atlantic Oceanic circulation in depth and isopycnic coordinates. *J. Phys. Oceanogr.*, **26**, 1849–1867.
- Cunningham, S. A., 2005: RRS Discovery Cruise 279, 04 Apr–10 May 2004: A transatlantic hydrographic section at 24.5°N. Cruise Rep. 54, 150 pp.
- , S. G. Alderson, B. A. King, and M. A. Brandon, 2003: Transport and variability of the Antarctic Circumpolar Current in Drake Passage. *J. Geophys. Res.*, **108C**, 8084, doi:10.1029/2001JC001147.
- Cuny, J., P. B. Rhines, and R. Kwok, 2005: Davis Strait volume, freshwater and heat fluxes. *Deep-Sea Res.*, **52**, 519–542.
- Danabasoglu, G., and J. C. McWilliams, 1995: Sensitivity of the global ocean circulation to parameterizations of mesoscale tracer transports. *J. Climate*, **8**, 2967–2987.
- Ganachaud, A., and C. Wunsch, 2000: Improved estimates of global ocean circulation, heat transport and mixing from hydrographic data. *Nature*, **408**, 453–458.
- Gent, P. R., and J. C. McWilliams, 1989: Isopycnal mixing in ocean circulation models. *J. Phys. Oceanogr.*, **20**, 150–155.
- Gloersen, P., and Coauthors, 1993: Arctic and Antarctic sea ice, 1978–1987: Satellite passive-microwave observations and analysis. NASA Special Publ. 511, 290 pp.
- Gordon, C., C. Cooper, C. A. Senior, H. Banks, J. M. Gregory, T. C. Johns, J. F. B. Mitchell, and R. A. Wood, 2000: The simulation of SST, sea ice extents and ocean heat transports in a version of the Hadley Centre coupled model without flux adjustments. *Climate Dyn.*, **16**, 147–168.
- Hallberg, R. W., and A. Adcroft, 2009: Reconciling estimates of the free surface height in Lagrangian vertical coordinate ocean models with mode-split time stepping. *Ocean Modell.*, **29**, doi:10.1016/j.ocemod.2009.02.008.
- Halliwell, G. R., 2004: Evaluation of vertical coordinate and vertical mixing algorithms in the Hybrid Coordinate Ocean Model (HYCOM). *Ocean Modell.*, **7**, 285–322.
- Houghton, J. T., L. G. Meira Filho, B. A. Callander, N. Harris, A. Kattenberg, and K. Maskell, Eds., 1996: *Climate Change 1995. The Science of Climate Change*. Cambridge University Press, 572 pp.
- , Y. Ding, D. J. Griggs, M. Noguer, P. J. van der Linden, and D. Xiaosu, Eds., 2001: *Climate Change 2001: The Scientific Basis*. Cambridge University Press, 944 pp.
- Hurlburt, H. E., A. J. Wallcraft, W. J. Schmitz, P. J. Hogan, and E. J. Metzger, 1996: Dynamics of the Kuroshio/Oyashio current system using eddy-resolving models of the North Pacific Ocean. *J. Geophys. Res.*, **101C**, 941–976.
- Johns, T. C., and Coauthors, 2006: The New Hadley Centre Climate Model (HadGEM1): Evaluation of coupled simulations. *J. Climate*, **19**, 1327–1353.
- Johns, W. E., T. J. Shay, J. M. Bane, and D. R. Watts, 1995: Gulf Stream structure, transport, and recirculation near 68° W. *J. Geophys. Res.*, **100C**, 817–838.
- Josey, S. A., E. C. Kent, and P. K. Taylor, 1998: The Southampton Oceanography Centre (SOC) Ocean—Atmosphere Heat, Momentum and Freshwater Flux Atlas. Southampton Oceanography Centre Rep. 6, 30 pp.
- Large, W. G., J. C. McWilliams, and S. C. Doney, 1994: Oceanic vertical mixing: A review and a model with a nonlocal boundary layer parameterization. *Rev. Geophys.*, **32**, 363–403.
- Levitus, S., and Coauthors, 1998: *Introduction*. Vol. 1, *World Ocean Database 1998*, NOAA Atlas NESDIS 18, 346 pp.
- Marsh, R., M. J. Roberts, R. A. Wood, and A. L. New, 1996: An intercomparison of a Bryan–Cox type ocean model and an isopycnic ocean model. Part II: The subtropical gyre and meridional heat transport. *J. Phys. Oceanogr.*, **26**, 1528–1551.
- Megann, A. P., and A. L. New, 1995: Meteorological Office/NERC agreement on “ocean modelling and parameterisation”: Isopycnic Development. Rep. 2: Intercomparison of quasi-global isopycnic and Cox models. Met Office, 16 pp.
- , and —, 2001: The effects of resolution and viscosity in an isopycnic-coordinate model of the equatorial Pacific. *J. Phys. Oceanogr.*, **31**, 1993–2018.
- New, A. L., and R. Bleck, 1995: An isopycnic model study of the North Atlantic. Part II: Interdecadal variability of the subtropical gyre. *J. Phys. Oceanogr.*, **25**, 2700–2714.
- , —, Y. Jia, R. Marsh, M. Huddleston, and S. Barnard, 1995: An isopycnic model study of the North Atlantic. Part I: Model experiment. *J. Phys. Oceanogr.*, **25**, 2667–2699.
- Qu, T., H. Mitsudera, and B. Qiu, 2001: A climatological view of the Kuroshio/Oyashio system east of Japan. *J. Phys. Oceanogr.*, **31**, 2575–2589.
- Roach, A. T., K. Aagaard, C. H. Pease, S. A. Salo, T. Weingartner, V. Pavlov, and M. Kulakov, 1995: Direct measurements of transport and water properties through the Bering Strait. *J. Geophys. Res.*, **100C**, 18 443–18 457.
- Roberts, M. J., R. Marsh, A. L. New, and R. A. Wood, 1996: An intercomparison of a Bryan–Cox type ocean model and an isopycnic ocean model. Part I: The subpolar gyre and high-latitude processes. *J. Phys. Oceanogr.*, **26**, 1495–1527.
- , and Coauthors, 2004: Impact of an eddy-permitting ocean resolution on control and climate change simulations with a global coupled GCM. *J. Climate*, **17**, 3–20.

- Sandwell, D. T., and W. H. F. Smith, 1997: Marine gravity anomaly from Geosat and ERS-1 satellite altimetry. *J. Geophys. Res.*, **102B**, 10 039–10 050.
- Sarmiento, J. L., N. Gruber, M. Brzezinski, and J. P. Dunne, 2004: High-latitude controls of thermocline nutrients and low latitude biological productivity. *Nature*, **427**, 56–60.
- Saunders, P. M., S. A. Cunningham, B. A. de Cuevas, and A. C. Coward, 2008: Comments on “Decadal changes in the North Atlantic and Pacific meridional overturning circulation and heat flux.” *J. Phys. Oceanogr.*, **38**, 2104–2107.
- Shaffrey, L. C., and Coauthors, 2009: U.K. HiGEM: The New U.K. High-Resolution Global Environment Model—Model description and basic evaluation. *J. Climate*, **22**, 1861–1896.
- Sloyan, B. M., and I. V. Kamenkovich, 2007: Simulation of Subantarctic Mode and Antarctic Intermediate Waters in climate models. *J. Climate*, **20**, 5061–5080.
- Solomon, S., D. Qin, M. Manning, Z. Chen, M. Marquis, K. B. Averyt, M. Tignor, and H. L. Miller, Eds., 2007: *Climate Change 2007: The Physical Science Basis*. Cambridge University Press, 996 pp.
- Stockdale, T. D., D. Anderson, M. Davey, P. Delecluse, A. Kattenberg, Y. Kitamura, M. Latif, and T. Yamagata, 1993: Intercomparison of tropical Pacific Ocean GCMs. World Climate Research Programme 79, WMO/TD-545, 43 pp.
- Sun, S., and R. Bleck, 2001a: Thermohaline circulation studies with an isopycnic coordinate ocean model. *J. Phys. Oceanogr.*, **31**, 2761–2782.
- , and —, 2001b: Atlantic thermohaline circulation and its response to increasing CO<sub>2</sub> in a coupled atmosphere-ocean model. *Geophys. Res. Lett.*, **28**, 4223–4226.
- , and —, 2005: Multi-century simulations with the coupled GISS-HYCOM climate model: Control experiments. *Climate Dyn.*, **26**, 407–428.
- , —, C. Rooth, J. Dukowicz, E. Chassignet, and P. Killworth, 1999: Inclusion of thermobaricity in isopycnic-coordinate ocean models. *J. Phys. Oceanogr.*, **29**, 2719–2729.
- Talley, L. D., 1996: Antarctic Intermediate Water in the South Atlantic. *The South Atlantic: Present and Past Circulation*, G. Wefer et al., Eds., Springer Verlag, 219–238.
- Trenberth, K. E., and J. M. Caron, 2001: Estimates of meridional atmosphere and ocean heat transports. *J. Climate*, **14**, 3433–3443.
- Valcke, S., L. Terray, and A. Piacentini, 2000: OASIS 2.4 user's guide. European Centre for Research and Advanced Training in Scientific Computing, TR/CGMC/00-10, 68 pp.
- Willebrand, J., and Coauthors, 2001: Circulation characteristics in three eddy-permitting models of the North Atlantic. *Prog. Oceanogr.*, **48**, 123–161.